ADDIS ABABA UNIVERSITY

ADDIS ABABA INSTITUTE OF TECHNOLOGY

SCHOOL OF CIVIL AND ENVIRONMENTAL ENGINEERING

Mix Design for Increasing the Earthquake Resistant of Circular Adobe Buildings

A Thesis in Structural Engineering

By Habtamu Hailemichael

December, 2021

Addis Ababa

A Thesis

Submitted in Partial Fulfillment of the Requirements for the Degree of Master of Science

The undersigned have examined the thesis entitled **'Mix Design for Increasing the Earthquake Resistant of Circular Adobe Buildings'** presented by **Habtamu Hailemichael**, a candidate for the degree of **Master of Science** and hereby certify that it is worthy of acceptance.

Dr.-Ing. Adil Zekaria		
Advisor	Signature	Date
your Internal Examiners' Name		
Internal Examiner	Signature	Date
your External Examiners' Name		
External Examiner	Signature	Date
Dean of schools' Name		
Chair person	Signature	Date

UNDERTAKING

I certify that research work titled "**Mix Design for Increasing the Earthquake Resistant of Circular Adobe Buildings**" is my own work. The work has not been presented elsewhere for assessment. Where material has been used from other sources it has been properly acknowledged / referred.

Signature of Student

Habtamu Hailemichael

ABSTRACT

Adobe buildings exist in different parts of the world and have been classified as unreinforced masonry structures. The construction technique of adobe is combining unfired clay mud and straw. The bricks are joined together with mortar made of mud and straw. This thesis studied the composition and mix ratio of soil to teff straw, which gave the maximum compressive strength by experiment. The result showed that the adobe prism specimen had a greater average confined compressive strength (987.66 KPa) compared with the same aspect ratio (1.66) in previous research. The prismatic specimens undergone consolidation at a higher strain range and further hardening of the prism makes the graph proportional (linear) before maximum stress is reached, after which the material was subjected to compression softening up to the ultimate strain sustained. Taking the maximum compression strength yielding mix ratio of 2:1 raw soil (58.9% of sand and 41.9% of silt and clay) to teff straw 'chid' (with lengths (cm) of 2-12, density (g/cm^3) (using water) 1.20, diameter (μm) 230–270, tensile strength (MPa) 280–326, and modulus (GPa) 9.2–10.7) produced small-scaled adobe brick for a circular model adobe building and tested the earthquake resistance with a static tilt table test. The table was modified by incorporating a double-acting electric-driven hydraulic cylinder jack to avoid irregular vibrations that would contribute uncounted force to the model. The model resisted the horizontal lateral force 187% more than the previous research without a crack, though it could resist more if the base restraint was designed well. The specimen of this thesis was subjected to an increasing roof pressure load of 2 kN/m^2 to 5kN/m^2 continuously on the same model, that could equivalently express the performance of the circular adobe building model with the pseudo-static analysis, could resist seismic with a PGA of 0.71 and 0.63 respectively.

Keywords: Adobe, teff straw, Static tilt table, circular adobe building,
earthquake resistance.

ACKNOWLEDGMENTS

All is for the one Who is of the whole, all goes to the almighty God to whom we are the witness through you everything is possible.

I Would like to express my sincere gratitude to my adviser, Dr.-Ing. Adil Zekaria, letting me do it which seems impossible then, for his invaluable supervision during the project's journey, which greatly aided in the project's completion and achievement at its best.

Selam children village ,Tsehay Roschlie Industrial and Agricultural Engineering, the company, the staffs specially at the hydra form production unit you deserve more than a word for providing working space and friendly cooperation when I am in need.

I can’t forget to offer my sincere thanks to **Artist Elias worku** (Senior Graphic designer) who was with me to the end helping me beyond the Photography.

My deep gratitude goes to Teklay T/Haymanot, Amare Chere, Tewodros Abraham, Lijalem Getachew, Bantider Baheru, Masresh Wondmu and those who are kind and assist me in the manufacturing, testing, and writing processes of the thesis.

Last but not least, I would like to thank my families for their unexpected understanding while I spent my full time to the project.

TABLE OF CONTENTS

LIST OF TABLES

LIST OF FIGURES

1 BACKGROUND

Adobe buildings exist in different parts of the world, which have been classified as unreinforced masonry structures. The construction technique of adobe is combining unfired clay mud and straw. The bricks are joined together with mortar of mud and straw. It is an ancient method of construction that dates back to 8000 B.C (Houben and Guillard 1994).

Adobe houses in the world is a historic building which also is the maximum proportion in number as a shelter for a human being. According to (Houben and Guillard 1994), 30% of the world's population lives in the earth- made constructions, with approximately 50% of them located in developing countries. Adobe constructions are very public in some of the world's most hazard-prone regions, such as Latin America, Africa, the Indian subcontinent, and other parts of Asia, the Middle East, and Southern Europe (M. G. Blondet 2003) .

The popularity of adobe buildings is due to their low cost and the lack of complicated skills like avoiding modern machinery. Also, it has better thermal capacity in hot or cold weather. The interior of an adobe home stays cool during hot summer days, and heat stays contained in a structure during a cold winter. It is a low fire risk and virtually sound proof (Hesham, et al. 2018). Adobe brick is an environmentally friendly product that reduces carbon footprint, but as the scarcity of construction materials escalates, green buildings like adobe brick will emerge inevitably.

Research from the seismic performance of adobe buildings and studies on the seismic retrofitting technique of historic adobe buildings based on the geometrical layout have indicated that buildings with a square plan had better seismic performance than rectangular ones, and buildings with a circular plan had better seismic resistance than square ones (Minke 2001).

Following the researcher's article (Jinwuth 2012), buildings with a heavier roof load and higher aspect ratios were more vulnerable to earthquake forces.

The static tilt-table testing confirmed a typical failure pattern of the circular adobe structures of cracking through the mortar and brick interface that causes a transverse tensile failure in-plane of its wall, which should happen to the structure in an actual earthquake (Jinwuth 2012) .

So, this thesis is imperative to improve the performance of adobe buildings by selecting the appropriate mix design which gives the maximum unconfined compressive strength. Furthermore, avoid the crack in the adobe buildings that forms the weak zone, in-plane, and out-off plane failure.

1.1 Statement of the problem

Currently, the deterioration of the environment is due to implementing industrially processed construction materials. Those materials emit toxins to the atmosphere and cause considerable damage to human life and its belongings.

According to scientists, replacing only 5% of concrete blocks used in the UK masonries with earthen masonry would mean reducing CO_2 emissions of approximately 100,000 tons (Morton, 2008) as cited in (Pacheco-Torgal 2015). Furthermore, the energy released for adobe production and its structure (Embodied energy) is the least from steel, concrete, or wood (Swan 2011).

Adobe structure is cheap, eco-efficient, and sustainable. It is estimated that clay and adhesive soil suitable for building use make up almost three-quarters of the earth's crust. Also, no need to transport it, which avert environmental pollution. However, 25 % of the world population does not have access to decent housing.

The weakness of adobe building is its susceptibility for seismic due to its poor mortar and adobe interface to mention some, in Peru /1970 and Bam, Iran /2003 more than 40,000 and 43,000 fatalities respectively.

The damage which destroyed dwellings in Pisco, Peru/2007 was 75,000 and 200,000 in El Salvador /2001.

Enhancing the in-plane shear and out-of-plane flexural strength mechanism is a vital means to protect human lives, preserve the ancient buildings and provide decent housing by studying different restoration techniques.

1.2 Objective

The purpose of this research is to examine and select the maximum unconfined compressive strength of adobe prism from different soil (sand, clay, and silt composition) and teff straw (chid) mixture (Adobe mix design). The mixture with the maximum strength is then used to study the behavior of circular adobe buildings under specified roof loadings with a static tilt table test which helps to enhance the failure of Adobe masonry during an earthquake and provide reliable design guidelines for the different builders and practicing engineers.

1.2.1 General Objective

- To investigate the performance of adobe in Circular adobe building for optimal mix design.

1.2.2 Specific objective

- To select the soil: composed of sand, clay, and silt; with straw (chid) ratio in the adobe, which gives the maximum compression strength of adobe prism.
- To investigate the circular adobe building seismic capacity (built of adobe with selected maximum strength) under specified loading with a static tilt table test at different tilting angles and the specified wall height.
- To make a comparison between the previously done researches with similar configurations of circular specimens.

1.3 Scope and limitation of the study

This research is limited to Adobe which is uncompressed and unstabilized with cement. Non-probable sampled soil, adapted by the local people the most, to reduce the number of samples. Gradation and sedimentation test has been done in the laboratory and on the field, respectively.

The failure angle is limited not only to the collapse of the model due to the expected crack but also to the restraint of the model base.

1.4 Method of the study

Prepared different mixes by varying the composition of the soil and straw here it is teff straw (chid) and produced five adobe blocks of size 100X200X300 mm^3 for each mixture.

Prism compressive strength test has been carried out and determined the maximum unconfined compressive strength of five batches of adobe mix, each with five specimens according to ASTM-C1314.

By picking the mix design that yields peak compressive strength adobe prism out of the five batches tested have produced the small-scale adobe brick and built the model on the tilt table.

The model is subjected to a constant acceleration (due to gravity) on a tilt table in this simple pseudo-static system.

The Static tilt table is produced by modifying the manual hydraulic jack with an electric-driven hydraulic motor to avoid the uneven uplifting force on the modified static tilt table. The adobe model was built on the table, and the applied pseudo-static force at failure has been determined via tilting angle at the failure.

1.5 Analysis of data

1.5.1 Data obtained from Soil gradation

The soil was selected and tested in the laboratory for sieve and hydrometer tests, and it was composed of 58.826% of Sand, 22.43% of Silt, and 18.74% of clay after the 7.46% Gravel has been distributed to sand, silt, and clay.

1.5.2 Data obtained from compression of Adobe Prism

From the graded and blended natural soil with the sand, five different mixture design has been prepared. Twenty-five adobe prisms constituted five from each mixture has been produced and tested for compression strength.

1.5.3 Data obtained from Model testing

The reduced scale (1/3) physical modeling has been used to investigate the earthquake performance of the adobe structure. The number of the static tilt table circular adobe model building test was one with the diameter of the wall 1.2 m, the thickness of the wall 0.066

m, the height of the wall 0.82m, and roof load of 2kN/m2 based on the maximum previous research.

1.6 Structure of the thesis

The following outline describes the general structure of the thesis: in Chapter 2, extensive literature research on the earthen construction, composition, properties, structural aspects, adobe code and guidelines, modeling, and previous research overview to give highlights on the subject matter.

Chapter 3, Presents the methodologies used to select the soil and laboratory testing for soil gradation. The production of adobe and its testing in the field and laboratory (prism compression, static tilt table test, and the steps used in the calculation) are also enumerated.

Chapter 4 highlights the analysis and result of the classification of the soil and compression test of the different mixture ratios made adobe prisms compression test to pick the peak design ratio.

The construction of the model and its shearing test using the static tilt table is also the development of Chapter 4 . Methods of loading and equivalency of the horizontal load to own weight also are compared with the previous research peak result keeping the other things constant.

Chapter 5 highlights a summary, recommendation, and conclusion of the research conducted in this thesis.

2 LITERATURE REVIEW

2.1 General

Adobe is a process that involves creating mud bricks with moulds but without compaction and drying them in the sun.

Adobe bricks have been around for thousands of years and are one of the first man-made building materials. The term "adobe" comes from the Egyptian word "thobe," which means "brick," and is derived from the Arabic word "ottob," which has been distorted into "adobe" in Spanish and "toub" in French. It's also known as 'banco' and sun-dried mud brick (Doat, et al. 1991) .

Due to the relative weights of the walls and simplicity in the method of construction researchers have kept their eye on adobe against other similar techniques of earth construction such as rammed earth, direct moulding, and Cob described in Table 2-1.

2.2 Earthen Construction

Earthen construction type, method, and constitutes (Table 2-1) may differ but, they are all simple, cheap, and sustainable. Without a doubt, one of the oldest building materials known to man is the earth. The Persians, Egyptians, Assyrians, and Babylonians all used it extensively. The examples that have come down to us show that our forefathers did not hesitate to use it in massive structures, such as the Ctesiphon arch in Iraq, or to entrust their most valuable possessions to it for all time, as the Egyptian (1^{st} dynasty) Pyramids and mastabas at Saqqarah demonstrate.

The increased interest in earth construction will be rapid due to the naturalness of the earth and the rapid rise in energy costs, which impacted materials like cement and burnt bricks. McKillop showed that although a burned brick requires two kwh of energy, a cement stabilized brick of the same size uses only 0.05 kwh. Recent analyses of "ecological costs" of construction methods that account for the "social cost" (maintenance of communication networks, social services, and so on) show that utilizing the lowest commercially available materials (cement mixtures) is not always the best long-term solution (Doat, et al. 1991).

Table 2-1 Different types of earthen construction

Earth cons.	**cob**	**adobe construction**	**Rammed-earth construction**	**Compressed earth block**
Constitute Material	a clayey sand mixed with straw	a clayey, sandy silt mix with or/ out straw or cement	Earth material without straw or fiber	
Method	laid up by hand continuously in a thick wall	cast in moulds and left to dry in the sun.	formwork similar to concrete cast-in-place wall construction	Similar to adobe with the blocks those are created under pressure
Size	often up to 610mm in thickness	differ	L=1600-4200mm H=800,t=486 mm	
reference	(Doat, et al. 1991)	(Bouhicha et al. 2005).	(Doat, et al. 1991)	(Morel et al. 2007).

2.3 Adobe building materials sustainability

Sustainable site materials and goods conserve natural resources, have a low environmental impact, pose no / minimal human and ecological health risks, and contribute to the execution of sustainable site projects.

According to Lippiat 1999, as referenced in Swan 2011, the building and construction industry consumes up to 40% of the world's energy and around 40% of its raw materials, although the structural system accounts for 25% of the building's overall environmental effect (Webster 2005) as cited in (Swan 2011).

Table 2-2 shows the material used in wall construction, the amount of energy required for these activities, and the material's disposal (known as embedded energy), in this process, energy is used and trash is produced in each of the construction phases though, to varying degrees.

Table 2-2 Embodied energy and the thermal resistance (R-value)of wall materials : Adapted from (Calkins 2009)

Walls material to enclose a floor area of 71:3 m2	**The roof system for the stud**	**embodied energy**	**The thermal resistance of a wall material (R-value)**	**Reference**
2.4 m high **straw bale** walls with stucco on both faces	a gable-style roof with 2 × 4 trusses at 600 mm on center, a 12.5 mm gypsum wall board ceiling, and R-44 blown cellulose insulation.	26,484 MJ	44.8 ft^2°Fh/Btu (RSI-value of 7.90 km^2/W)	(Pierquet ,1998)
2 × 6 **wood-frame** walls clad in vinyl siding		33,314 MJ	22.2 ft^2°Fh/Btu (RSI-value of 3.91 km^2/W)	(Pierquet ,1998)
A stabilized compressed earth block, mortar,and stucco wall		13,213 MJ	-	(Venkatarama Reddy, 2003; Shukla ,2009)

Table 2-2 shows the stabilized compressed earth block is with the least embodied energy. If it were for the unstabilized and uncompressed, it would be almost null, which completely fulfills the criteria for sustainability as shown in Table 2-3 since it minimizes resource use, has a low environmental effect, poses no health risk, and helps sustainable site design strategies.

Besides structural issues, future construction materials should have to meet the highest level of sustainability as tabulated in Table 2-3 for the well-being of the dwellers.

Table 2-3 Materials for Sustainable Sites Defined: Adapted from (Calkins, 2009)

Materials or products			
That minimize resource use:	**With low environmental impacts:**	**Posing no or low human and environmental health risks**	**That assist with sustainable site design strategies:**
• Products that use less material • Reused material and products • Reprocessed materials • Post-consumer recycled-content materials • Products made from agricultural waste • Materials or products with reuse potential • Materials or products with recycling potential • Renewable materials • Rapidly renewable materials • Durable materials • from manufacturers with product take-back programs	• Sustainably harvested or mined • Minimally processed • Low-polluting in extraction, manufacture, use, or disposal • Use low water in extraction, manufacture, use, or disposal • Use low energy in extraction, manufacture, use, or disposal • made with energy from renewable sources (e.g., wind, solar) • Local materials	• Low-emitting • Avoid toxic chemicals or by-products in their entire life cycle	• Promote a site's hydrological health by reducing storm water runoff quantities and improving hydrologic qualities • Reduce the urban heat island effect • Reduce energy consumption of site operation • Reduce water consumption of site operation

2.4 Composition and Properties of adobe

2.4.1 Composition of Adobe brick

The mix ratio of adobe, especially unstabilized and uncompressed, varies from place to place even in similar regions due to the composition of the constituent materials of the soil available, the straw type, and the ratio used which make the adobe. Also, to some extent, the water content, the drying process, and duration impact it.

According to (Lisa and Vince 2010) The best adobe combination for workability and durability is around 75 percent sand and 25 percent clay by volume, with just enough water to reach the desired consistency.

There are no precise standards and codes written about uncompressed, unstabilized adobe masonry that specify the experimentally approved mixture design. So, a study from scratch is needed.

It is required to examine the properties and composition of the soil with the maximum strength output mix ratio to advance the usage of earthen material to a modern and sustainable future.

2.4.1.1 Classified soil type and compressive strength

The effect of material composition with the compression strength test (Dhandhukia, et al. 2013) is shown in the Table 2-4 and figures 2-1 to figure 2-4.

Table 2-4 Analysis of physical properties of soil and its classification using Unified and ASTM D3282 classification

Soil type	Collection site	Grain size analysis			Atterberg limit (%)			Unified classification		ASTM D3282	
		Gravel (%)	Sand (%)	Silt + Clay (%)	LL	PL	PI	Group symbol	Group name	Group	Significant material
EB1	Dry pond surface soil at Karoli	0	51	49	23	22	1	SM	Silty sand	A4	Silty soil
EB2	Dry pond 6 mt deep soil at Karoli	0	53	47	23	22	1	SM	Silty sand	A4	Silty soil
EB3	Little Rann of Kutch	0	19	81	61	20	41	CH	Clay of high plasticity, fat clay	A-7-6	Clayey soil
EB4	Black cotton soil from Bhimnath, Bhavnagar	12	24	64	42	22	20	CL	Clay	A-7-6	Clayey soil
EB5	Charusat campus Nr. R&D center	0	31	69	26	24	2	ML	Silt	A4	Silty soil
EB6	Narmada River Bed, Bharuch	0	16	84	24	22	2	ML	Silt	A4	Silty soil
EB7*(9:1)	10%	3	35	62	25	22	2	ML	Silt	A4	Silty soil
EB8* (8:2)	20%	0	32	68	27	21	6	CL–ML	Clayey-silt	A4	Silty soil
EB9* (7:3)	30%	1	36	63	26	22	4	ML	Silt	A4	Silty soil
EB10* (6:4)	40%	0	38	62	28	22	6	CL–ML	Clayey-silt	A4	Silty soil
EB11* (1:1)	50%	0	32	68	28	21	7	CL	Clay	A-7-6	Clayey soil
EB12	Bharuch yellow soil	0	59	41	28	27	1	SM	Silt	A4	Silty soil
EB13	Changa farm soil	0	54	46	24	21	3	SM	Silty sand	A4	Silty soil

EB7, EB8, EB9, EB10, EB11 these 5 soil types were prepared by mixing EB1 and EB4 in the ratios of 1:9, 2:8, 3:4, 4:6 and 5:5 respectively.

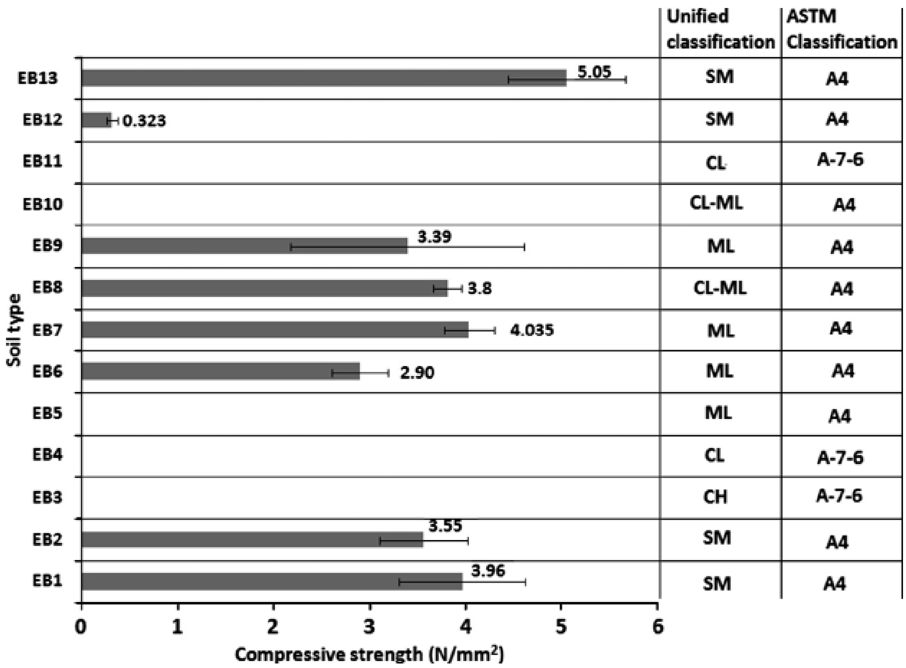

Figure 2-1 The correlation between classified soil types with compressive strength

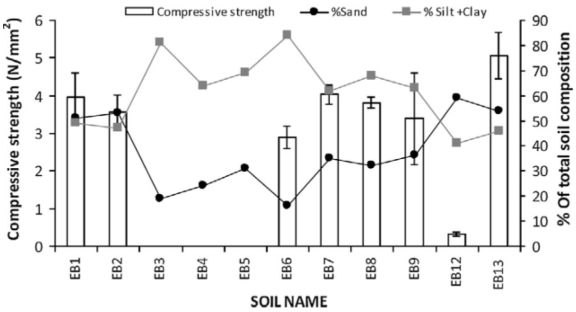

Figure 2-2‘Correlation between soil compositions with compressive strength of bricks.

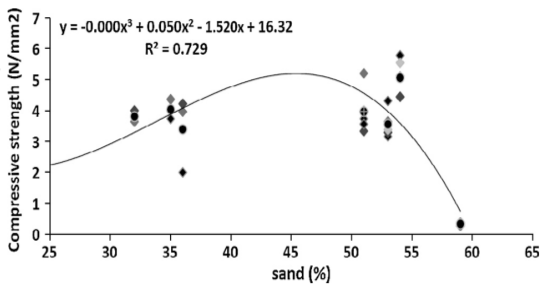

Figure 2-3 Sand content Vs compressive strength of bricks

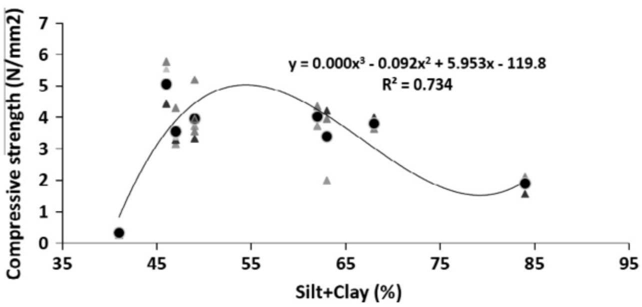

Figure 2-4 Correlation between silt + clay content with compressive strength of bricks

2.4.1.2 Atterberg's limit and compressive strength of the soil correlations

The effect of soil type composition and properties with the compression strength test (Dhandhukia, et al. 2013) is shown in the Figure 2-5 to Figure 2-7. In these figures the ordinates are the compressive strength and the abscissa are the liquid limit, Plastic limit and Plasticity index respectively.

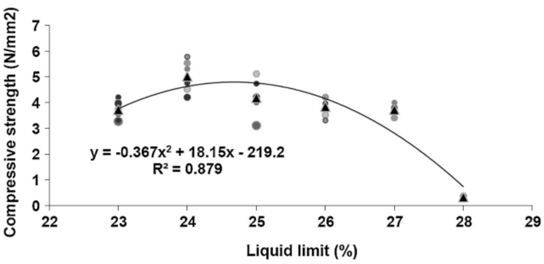

Figure 2-5 Correlation between Liquid limit (LL%) with compressive strength of bricks

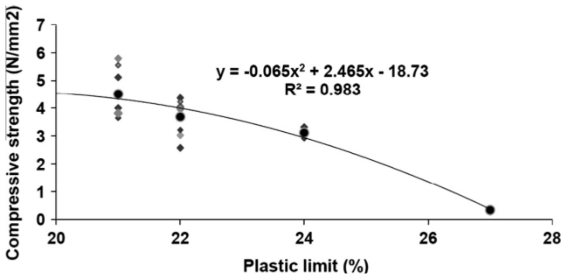

Figure 2-6 Correlation between Plastic limit (PL%) with compressive strength of brick

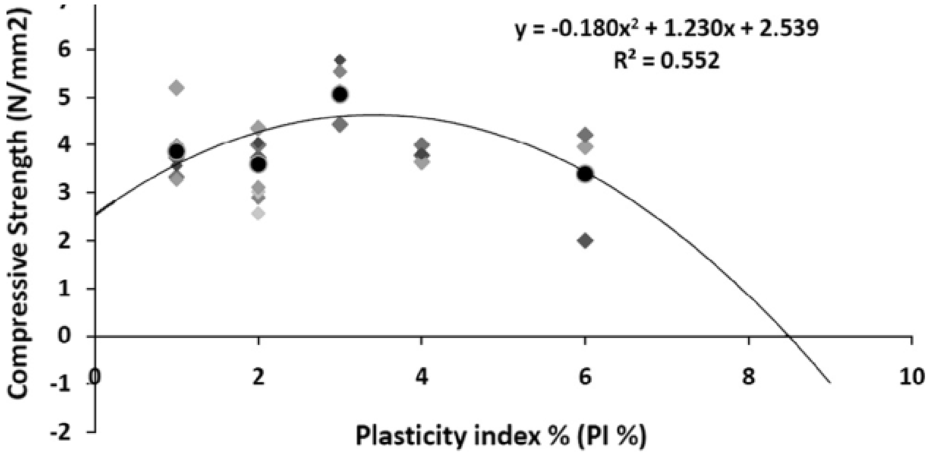

Figure 2-7 Correlation between Plasticity Index (PI%) with compressive strength of bricks. (-▲-, and ---●- indicates the arithmetic mean of the values)

2.4.1.3 Straw as a control of microcracking and stabilization

Some soils that are considered inappropriate for earthen construction can be modified with stabilizers to make them suitable. Mechanical (e.g., compacting), physical (e.g., adding fibers or minerals), or chemical (e.g., cement, lime, or asphalt emulsions) stabilization are the different options (Houben and Guillard 1994),as cited in Calkins,2009).

Starting from the early 3500 years AD, the straw, a by-product of harvested grain, has been used to construct earthen buildings (Bible n.d.).

The use of straw as a stabilizer is essential for strong adobe masonry construction. It controls microcracking of the soil mortar owing to drying shrinkage. Micro cracking caused by drying shrinkage can also be reduced by adding coarse sand to the mixture (Blondet et al. 2011) . The maximum amount of straw that has to be added to the soil should be workable.

From on-site measurement and (Devnani and Sinha 2018) , the teff straw 'chid' were had lengths (cm) of 2-5, density (g/cm^3) (using water) 1.20, diameter (μm) 230–270, tensile strength (MPa) 280–326, and modulus (GPa) 9.2–10.7.

2.4.2 Properties of Adobe brick

2.4.2.1 Physical Properties of Adobe Brick

a) Dimension

The dimension of the adobe block varies since there is no internationally accepted standard size and the different types of raw material used in various places but can be categorized in the threshold depending upon the literature.

"Some reported dimensions of adobe in historic structures have ranged from 9x5x5 inches (23 x 13 x 13 cm) to 16 x 5 x 5 inches (41 x 13 x 13 cm)" (Steen 1971) as cited in (Clifton 1977).

b) Density

Reported values of the density (Clough 1950, Eyre 1935, Schwalen 1968, and Webb, Cilliers, and Stutterheim 1850), as cited in (Clifton 1977) of dried adobe brick range from 98 to 125 lb/ft (1570 to 2000 kg/m^3) and increase with higher sand contents.

c)Coefficient of thermal expansion

Eyre (Eyre 1935), as cited in (Clifton 1977) reported that the coefficient of thermal expansion for adobe brick made from 5 different soils ranged from 0.90 x 10-6 to 3.0 x 10-6 in/in per °F (0.50 x 10-6 to 1.7 x 10-6 cm/ cm per °C). Webb (Webb et al. 1950), as cited in (Clifton 1977),found that the coefficients of thermal expansion of adobe bricks made from 40 different soils ranged from 11.1 x 10-6 to 14.2 x 10-6 per °C. The reason for the large differences between the two sets of data is not clear.

d)Thermal conductivity

Whittemore (Whittemore et al.,1941), as cited in (Clifton 1977),reported that adobe brick and rammed earth have thermal conductivities (K) of 10.7 and 11.3, respectively, this shows, the value of conducting heat is higher than the other common building material, for example the thermal conductivities (K) of concrete varies from 6 to 9 (Clifton 1977).

e) Permeability

Whittemore (Whittemore et al.,1941), measured water permeability using a water flow rate of 40gal/hr (.15m^3/hr). They observed that in about 0.03 hr, water was visible on the back surface of a 12 inch (30cm) thick adobe brick wall. Therefore, it needs some mechanisms to stabilize it to increase the time required for penetration.

The capillary rise of water in adobe mixed with 10 percent by weight of Portland cement was 3.18 cm in ten minutes, compared to 1.4 cm in the unadulterated adobe. However: it is well-documented that the addition of Portland cement to soil has a positive effect on the resistance of adobe brick to water damage (Fenton 1941, Whittemore et al.,1941, Smith 1974), as cited in (Clifton 1977).

According to Crocker (Crocker 2001) the Portland-stabilized blocks proved to be just as brittle as the normal kind during an earthquake due to the interface between hard and soft materials. It's a loss. Also, building that has been accumulating moisture for years because it is plastered with Portland cement may be at the peak of their vulnerability.

2.4.2.2 Mechanical properties of Adobe brick

i) Compressive strength

The literature provides a wide range of compressive strength values for cured adobe bricks. However, it was suggested that prisms with a slenderness ratio (Hight to thickness ratio) of 1:4 be tested. It was also revealed that the age of the specimens could be of significant effect; nevertheless, more research into this topic is needed.

According to preliminary findings shown in Table 2-7 in which the mean value of Table 2-6 is included, the compression strength of 1:4 slenderness prisms range between 0.80 and 1.20 MPa, depending on the specimen age (Sabino and Tarque 2011) .

Factor affecting Compressive strength

a) Curing time

Adobe brick compressive strength rises with age, according to Webb (Webb et al. 1950), as referenced in (Clifton 1977). If the adobe brick was in a "wet state," its 28-day strength fall (The word "wet state" was not defined, and there's no guarantee that the condition of the environment was well-controlled).

b) Moisture of the storing condition

Due to the weakening of binders by water and the creation of pore water pressures, strength decreases as moisture content rises. When saturated, the compressive strength of plain soil, which has not been stabilized, is zero. (Walker 1995) and Moisture content of un-stabilized materials during testing should ideally mirror in-service circumstances.

c) Composition of the soil

It was revealed that the 28-day compressive strength of adobe soil increases with increasing clay concentration until the optimal clay content is achieved, beyond which shrinkage cracking causes a loss in strength (Clough 1950), as cited in (Clifton 1977). The effect of the clay content on the strength of the adobe brick appears to reduce over time as the adobe brick ages (Patty,1936), as cited in (Clifton 1977). The compressive strength of the soil increases slightly with its fineness (Eyre 1935), as cited in (Clifton 1977).

d) The amount of mix water used in making the adobe brick

It has been proven that the ideal amount of mixing water for each adobe soil that produces the best strength and density can be found experimentally (Webb et al., 1950, Fenton 1941), as cited in (Clifton 1977).

e) Density of the dried brick,

The highest density depends on the amount of mixing water used for each soil to produce the adobe. It has been possible to get rather direct relationships between the densities of dry adobe bricks and their compressive strengths (Schwalen 1935), as cited in (Clifton 1977).

f) The size of the test specimens.

According to Schwalen (Schwalen 1935), as cited in (Clifton 1977) it is known that the size of the specimen affected the compressive strength. Table 2-5 Summary of existing results from compressive tests of various size adobe specimens.

It is all about that the force opposing lateral expansion increase as the specimen's height-to-width ratio decreases. For instance, reducing test specimens from prisms 15 x 15 x 7.5

cm to prisms 10 x 10 x 7.5 cm resulted in an average 11 percent reduction in measured strength. When the test specimen size was reduced from 29.69 x 38.74 x 12.54 cm to 29.37x 18.89 x 12.54 cm, the measured compressive strength was reduced by approximately 50% (Whittemore et al. 1945), as cited in (Clifton 1977).

The requirement for a consistent specimen size for testing the compressive strength of adobe bricks is evident from these findings (Clifton 1977). Table 2-6 and 2-7 shows varying strength for various adobe prisms size specimens.

Table 2-5 Summary of existing results from compressive tests of various adobe specimens.

Sample size (mm)	**Aspect ratio**	**Mixture (%) by volume**			**Curing Months (T0 and Hum)**	**Compressive strength (MPa)**	**Cov(%)**	**Reference**
	H/W	**Clay /silt**	**Sand/Gravel**	**Straw fiber**				
230 × 150 × 130 (Eight block for each ten mixture)	0.9	9.7/16.4	40.3/25.8	0.2	2(26^{0}C, 47%)	2.14	8.5–26	(Quagliarini and Lenci 2010)[1]
	0.9	25.6/43.6	11.4 /9.3	0		2.88		
50 × 50 × 50 cube (45 cubes for 11 mixture/setup)	1	78-91	8-18/1-4	20–40	>1	1.39-1.75	11.	Specimens cut from adobe bricks in dry conditions, by (Rogiros, et al. 2014)[2]
	1	61-86	11-26/3-13	15–28	Ditto	0.6 -1.47	22-76	
Cylinders H=Dia.=50mm (86 brick for 14 mixture/setup)	1	78-91	8-18/1-4	20–40	Ditto	1.13-1.41	20-27	
	1	61-86	11-26/3-13	15–28	Ditto	0.76-1.06	2-17	
100 × 100 ×50 Prism,92 prism of 25setup/mixture	0.5	78-91	8-18/1-4	20–40	Ditto	0.73-2.47	12-42	
	0.5	61-86	11-26/3-13	15–28	Ditto	0.45-3.31	4.3-23	
200 × 90 × 50 Prism (6prism for each 4 mixture)	4	By weight			>1	1.70	17	(Feng, Gang, et al. 2013)[3]
		49	49.5	0.5				
	4	40	59.5	0.5	>1	1.39	8	

1)As fiber content increases, compressive and tensile strengths decrease, and shrinkage rates decrease.
2)The response of adobes in compression strongly depends on the form (cube, cylinder, prism) and size of the specimen examined.
3) Once the **aspect ratio exceeds four**, platen restraint influence on measured strength can be effectively reduced.

Table 2-6 Results of compression tests on adobe prisms carried out by Blondet and Vargas [1978]

ID	Dimension (m)	Maximum load (kN)	Compression strength (MPa)	Reference
C-1	0.19 x 0.385 x 0.79	62	0.85	compression tests on adobe prisms carried out by Blondet and Vargas [1978]. The bricks were made of clay soil mixed with straw, and dried under the sun for approximately 2 weeks, had a constant slenderness ratio 1:4 and were tested after one month construction.
*C-2	0.20 x 0.40 x 0.80	59	0.74	
C-3	0.20 x 0.39 x 0.80	62	0.8	
C-4	0.195 x 0.39 x 0.785	57	0.74	
C-5	0.195 x 0.39 x 0.80	65	0.86	
C-6	0.20 x 0.39 x 0.79	65	0.83	
C-7	0.19 x 0.39 x 0.79	62	0.84	
C-8	0.20 x 0.40 x 0.80	59	0.73	
C-9	0.195 x 0.39 x 0.80	66.25	0.87	
C-10	0.195 x 0.39 x 0.785	65	0.85	
C-11	0.195 x 0.39 x 0.78	73	0.96	
C-12	0.195 x 0.39 x 0.785	70	0.92	
		Mean	**0.83**	

Table 2-7 Results of compression tests on adobe prisms carried out by Vargas and Ottazzi [1981]

ID	Slenderness	Mean Maximum load (kN)	Mean Compression strength (MPa)	Age in months	number of test specimens	Reference
J	1:1 (2 bricks)	94.13	1.18	1	8	adobe prisms carried out by Vargas and Ottazzi [1981].
I	1:1.5 (3 bricks)	68.2	0.85	1	10	
H	1:2 (4 bricks)	62.97	0.79	1	10	
G	1:3 (6 bricks)	64.25	0.80	1	9	
C	1:4 (8 bricks)	63.98	0.83	1	12	
K	1:5 (10 bricks)	61.8	0.73	1	10	
CP3	1:4 (8 bricks)	96.2	1.20	11	7	
CMB	**1:4 (8 bricks)**	**97.6**	**1.22**	**7**	**23**	

ii) The tensile strengths of adobe

Because of the effects of shrinkage cracks, the tensile strengths of adobe are very low and difficult to measure precisely. The reported values vary from 54 to 121 psi (0.37 to 0.834 MN/m^2), with a ratio of roughly six (6) between compressive and tensile strengths (Eyre 1935), as cited in (Clifton 1977). Adobe brick with low flexural strengths is produced generally by soils with high clay content as reported by (Clough 1950), as cited in (Clifton 1977).

iii) Elasticity modulus /Young's Modulus /

Given the granular structure of earthen materials, it may be argued that elasticity has no physical significance in adobes. In actuality, due to the collapse of air-voids within the soil matrix and irreversible sliding/displacement of the soil grains, the commencement of non-linear response will occur at an extremely low level of stress (Meyer, et al. 2013)and (Hakimi, et al. 1999). Therefore, the elastic modulus in compression can be considered as a stiffness parameter rather than an indicator of actual material linearity.

In a few published literatures, researchers like (Kouakou and Morel 2009) show the determination of the elastic modulus of earthen specimens of different compositions and its correlation with the physical and mechanical properties.

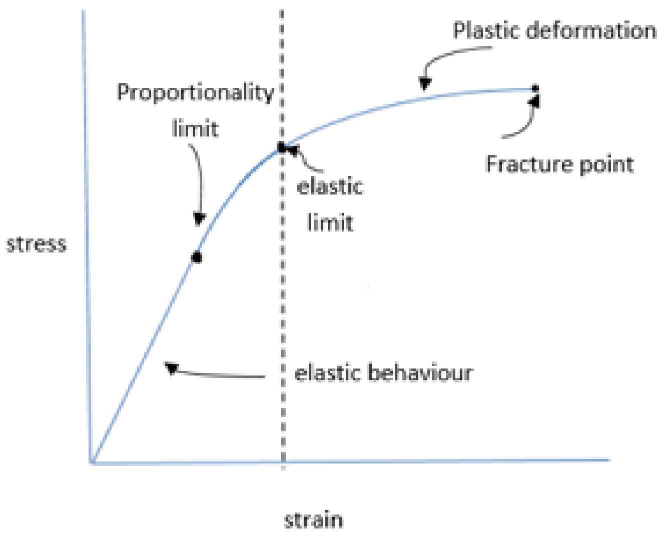

Figure 2-8 stress -strain relationship

a) Young's modulus, according to (ASTM-E111–04 2010).

Young's modulus is calculated by the slope of the line for forces less than the proportional limit figure 2-8. The lower force point is determined by the limits given in ASTM E111-

04, Section 8.1. (2010). The following equation is used to compute Young's modulus from the force increment and corresponding extension increment between two points on the line as far apart as possible:

Young's modulus =A /[(A/B)+ C]

where:

A = stress increment,
B = trial modulus, and
C = deviation increment.

It is suggested that the strain corresponding to the spacing of the parallel lines be reported as measure of the variability of the data (ASTM-E111–04 2010).

b) Elasticity modulus, according to (Blondet and Vargas 1978).

The elasticity modulus was calculated by taking 50% of the maximum compression load and its corresponding deformation from the elastic region of the stress-strain curves. (Blondet and Vargas 1978).

C) By using Chord modulus according to (ASTM-E111–04, 2010).

Chord moduli have been computed over the gradient of the curve by drawing a line which best fit the curve increasing section of the stress–strain curves, which is between any two stresses.

2.5 Previous research related to the Seismic performance of Earthen Buildings

Researches were carried out to assess the seismic performance of earthen material with a model, full-scale building, and retrofitting of the existing earthen houses.

The performance of the earthen buildings has experimented with the method of physical modeling and finite element model simulation, wherein the physical modeling of the full scale and the reduced scale model is examined by the static tilt table, dynamic shaking table, and pushover testing.

Additionally, some qualitative and quantitative description of the seismic performance of existing adobe buildings has been studied by official pre-earthquake housing statistics and official post-earthquake damage statistics taken.

In this section, previously studied researches regarding the seismic performance of earthen buildings generally and the circular adobe buildings specifically tested on a static tilting table will be mentioned.

2.5.1 The use of static tilt-table testing methods to evaluate and improve researches related to the seismic performance of adobe structures or other circular elements.

a) Study into the Earthquake Resistance of Circular Adobe Buildings using Static Static tilt Tests . PHD research conducted In Perth, Western Australia: (Jinwuth 2012)

This work details a series of tilt table tests that were carried out to investigate the performance of unreinforced circular adobe constructions to earthquake stresses. Before constructing the model, the specimen adobe prism was tested for compression strength as shown in Table 2-8.

Table 2-8 Results from compression tests of adobe prisms **(Jinwuth 2012)**

Specimen	**H/T ratio**	**Surface Area** (m^2)	**Max Load P** (*kN*)	**Prism Strength** f_c (*kPa*)	**Unconfined Compressive Strength*** (*kPa*)*****
C1	1.65	0.035	31	885.7	669.8
C2	1.68	0.033	31	939.4	713.8
C3	1.7	0.035	28	800	609.8
C4	1.67	0.034	29	852.9	647
C5	1.71	0.033	30	909	694
Average	1.68	0.034	29.8	877	666.9
SD	0.02	0.001	1.30	53.6	40.6
CoV (%)	1.0	3.0	4.0	6.0	6.0

Notes:
SD = Standard Deviation
CoV = Coefficient of Variation
* Determine the aspect ratio correction factor from AS 3700 (Australian Standard)

Nine small-scaled (1:3 scale) adobe structures with various layouts and roof loads were built, as the relationship between prism strength and unconfined compressive strength is illustrated in Table 2-9.

Table 2-9 Small scale adobe models: specifications (Jinwuth 2012)

Model Set	***Wall Thickness* (mm)**	***Diameter (m)***	***Wall Height* (m)**	***Roof Height* (m)**	***Roof Load Pressure* (kN/m^2)**	***Total Roof Load* (kN)**	***Total wall load* (kN)**
1A	**31**	**1.2**	**0.82**	**0.94**	**2**	**2.25**	**1.56**
2A	**31**	**1.2**	**0.82**	**1.00**	**3**	**3.38**	**1.55**
3A	**31**	**1.2**	**0.82**	**1.06**	**4**	**4.51**	**1.55**
2B	**45**	**1.2**	**0.82**	**0.94**	**2**	**2.25**	**2.23**
3B	**60**	**1.2**	**0.82**	**0.94**	**2**	**2.25**	**2.93**
2C	**31**	**1.4**	**0.82**	**0.94**	**2**	**2.25**	**1.82**
3C	**31**	**1.0**	**0.82**	**0.94**	**2**	**2.25**	**1.29**
2D	**31**	**1.2**	**0.96**	**1.08**	**2**	**2.25**	**1.82**
3D	**31**	**1.2**	**0.67**	**0.79**	**2**	**2.25**	**1.27**

Figure 2-9 Tilting the specimen until cracking and subsequent failure (Jinwuth 2012)

Table 2-10 Results of the static tilt testing nine circular adobe models (Jinwuth 2012)

	CASE #1A	***CASE #2A***	***CASE #3A***	***CASE #2B***	***CASE #3B***	***CASE #2C***	***CASE #3C***	***CASE #2D***	***CASE #3D***
First crack Angle (degrees)	**29**	**25**	**21**	**30**	**32**	**31**	**29**	**28**	**34**
Horizontal force (*kN*)	**1.85**	**2.08**	**2.27**	**2.24**	**2.75**	**2.15**	**1.55**	**1.72**	**1.91**
horizontal force compared to model own weight (%)	**48.5**	**42.2**	**37.4**	**49.9**	**52.9**	**52.9**	**43.8**	**42.2**	**54.5**

The result from the test, as shown in Table 2-10. depicts buildings having a heavier roof load, with higher aspect ratios were shown to be more sensitive to earthquake effects in the study by (Jinwuth, Study into the Earthquake Resistance of Circular Adobe Buildings using Static Static tilt Tests 2012).

Following this research, a static pushover test and two shaking table tests were also performed to assess the accuracy (reliability) of the predictive model derived from the tilt table tests.

Static Pushover testing

This test determines the predicted seismic force and deformation of the structure undergone in the university of Technology Sydney. The selected model (Specimen 1A) was pushed to total collapse by a static lateral load to get valuable information on the tested wall deformation and the failure loading of the model.

Figure 2-10 Failure crack patterns at the southwest and southeast side wall (Jinwuth 2012)

Reliability of Static tilt table testing

The outcome from the pushover test in which the crack of the specimen starts when the load reached 1.87 kN and failed when the load reached 2.05 kN showed a similar result as the tilt table test, first cracking appeared when the horizontal load became 1.85 kN and the total failure occurred at a load of 2.02 kN shown in Table 2-11. This test has validated the reliability of the static tilt table.

Table 2-11 Result of identical model tested with static tilt table and pushover test

Test Type	Loading		
Static Tilt Table (on Model 1A)	**mg sin(θ)** (the horizontal load) reached		
	1.85kN		2.02 kN
Pushover Test (on similar Model to 1A)	**Push-Loading**		
	1.87kN	1.9kN	2.05kN
Failure Status	The first visible shear cracking occurred at the top	Transverse to the direction of applied force	The critical failure cracking occurred

It has to be emphasized that pushover testing is done with static loads. As a result, some significant deformation modes that may occur in a structure subjected to actual earthquakes may go undetected. So, more experiments were carried out, including some limited dynamic testing of models on the University Technology Sydney (UTS) displacement-driven shaking table.

Shaking table test

Four earthquake recordings were used to simulate a succession of seismic ground motions. For the time-scaled input motion, the simulations were run with varied acceleration intensities, ranging from 20% to 140 % for the El Centro earthquake, 60% for the Northridge and Kobe earthquakes, and 40% to 120 % for the El Salvador earthquake.

During the simulation S13(100%) (13th Simulation with an intensity of 100%), which was equal to 0.74g for the PGA, the specimen (model 1A) appeared to display the first visible cracking (Jinwuth 2012).

It was also reported that the shaking table testing revealed the same shear crack characteristics as the tilt testing.

This research deals with an experimental comparison of two symmetrical shapes of unreinforced adobe walls, namely a square and a circular model. According to the output data, the circular structure performed better in these compared studies.

2.5.2 static tilt-table tests of adobe models research conducted on earthquake resistant earthen buildings by the Pontificia university in Peru (PUCP).

The results of these experiments are of high quality. However, there is a scarcity of quantitative data on pre-test processes and post-test analysis in the research report.

a) In 1972, following the 1970 Huaraz earthquake Mw 7.8, around 70 000 persons died. These fatalities and damage aroused awareness in Peru about the necessity to research the problem of adobe construction strength to seismic, and then the first simple experiment was undertaken at PUCP.

The researchers discovered that a vertical inside cane reinforcement (reinforcement from the stem of the cane), along with horizontal crushed cane every fourth row of adobe bricks, considerably increased the seismic strength of the housing models in these static tests. Cane reinforcement substantially resists twice the maximum horizontal load capacity and nearly six times the lateral deformation compared to unreinforced walls. With the proposed modification, the static seismic coefficients were enhanced from 0.23 g to 0.42 g. The ability of a wall to maintain its stability after significant crack was investigated in this study when it was reinforced with a mesh of the interior of the cane (Blondet and Garcia 2003). The monotonic lateral load testing of full-scale walls likewise confirmed the stability .

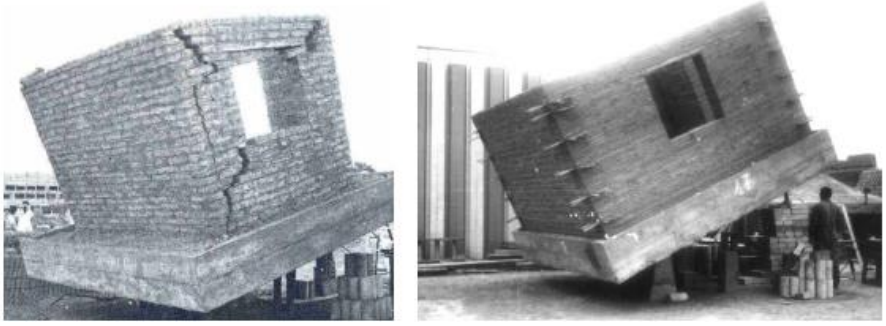

(a) Unreinforced specimen b) Test specimen strengthened with cane reinforcement

Figure 2-11 Seismic Performance of an Unreinforced and a Strengthened Adobe Building in PUCP (Blondet and Garcia 2003).

b) In 1979, the PUCP and the National Autonomous University of Mexico (UNAM) collaborated to design the next adobe masonry research project .

For dynamic testing of wall panels and model buildings, a 4 m x 4 m uni-axial shaking table was utilized in order to simulate the earthquake. Most simulations used the temporal history of the 1970 Huaraz earthquake with intensity scaling of ground motion to examine the behavior of structures under dynamic load situations. Adobe specimens were also subjected to property tests, such as axial compression, indirect tension, diagonal compression, and full-scale shear tests were performed on adobe specimens (Blondet et al.2002) as cited in (Jinwuth 2012).

c) Torrealva, Vargas, and Blondet conducted seismic simulation tests on full-scale adobe models at PUCP in 1984. Full-scale models with and without interior cane reinforcement were subjected to increasing amplitude seismic motions using the time history from the Huaraz earthquake of May 31, 1970. According to the majority of results from these tests, the internal cane reinforcement with a wooden ring beam prevented wall separation and out-of-plane failure.

d) In 1992, the adobe research team at PUCP undertook dynamic testing of full-scale adobe models to improve adobe constructions. Eight full-size models of a one-room single-story building with varying construction techniques were shaken with increasing intensity on the shaking table. The primary findings were that improving the adobe construction process increased the wall resistance and rigidity on its own. The results reveal that horizontal and vertical cane reinforcement, combined with a solid ring beam, can prevent wall separation in the corners while also preserving the structure's integrity even after the walls have been severely damaged (Blondet and Brzev, 2003).

2.5.3 Tilt-table-testing of the FUNDASAL

(Salvadoran Foundation for Development and Minimum Housing)**, El Salvador**

The models were made entirely of the same material for brick and mortar with a clay to four sand ratio (1:4) and were completely solid (no doors or windows). They were 6.00 meters long, 3.50 meters wide, and 2.28 meters high. The findings of these studies led to advancements in traditional house construction technologies. Two adobe houses; one unreinforced and the other with bamboo reinforcement and wall buttresses, were built to evaluate their seismic resistance using a static method on a tilt table as shown in Table 2-12 (Pena and Lopez,2007), as cited in (Jinwuth 2012).

*a)*Tilt table with 40 degrees as maximum angle b) reinforced wall tilted

Figure 2-12 static tilt table test of reinforced rectangular adobe house

When the horizontal force equivalent was 24 % of its own weight, the typical adobe structure collapsed, whereas the reinforced house collapsed at roughly 50 %. Tension in the corners of the out-of-plane wall caused the traditional building to fail, but the strengthened house showed flexural cracking in the out-of-plane walls.

The following lists are some of the seismic performance tests for adobe buildings using a shaking table with the previously recorded earthquake simulation to get a rational design proposal for the seismic design of confined adobe buildings.

i. Experimental research and seismic design proposal for confined adobe masonry by Catholic University of Peru, (San, et al. 2013).
ii. Seismic improvement of adobe-mud brick walls -comparison between internal and external vertical reinforcement by the university of technology, Sydney (Dowling n.d.).
iii. Shake table testing of scaled geogrid-reinforced adobe wall models (Tipler, et al. 2010)
iv. Static and dynamic testing of adobe-mudbrick structures (Samali, Dowling and Li 2015).
v. Seismic performance of traditional adobe masonry walls subjected to in-plane cyclic loading (Feng, Wang, et al. 2016).

2.6 Structural Aspect of Adobe Houses

The kind of application, performance requirements, construction method, climatic and seismic characteristics of the site is all critical structural concerns for earth structures.

The majority of sources of knowledge on the structural design of earth structure focus on building structures, not retaining walls, freestanding walls, or pavements (Calkins 2009).

The important thing should be improving the soils for earthen construction to attain the maximum possible compressive strength and formulating a code for a suitable combination of soils.

Adobe buildings, besides other types of earth buildings, starting from early human civilization, have been used as a shelter. It will be the future most suitable due to environmental and other issues described in section 2-3. But needs more intensive researches on earthen material and structures to be back to the earth!

2.7 Codes, Guidelines and Standards

Earthen building systems have never been engineered before, but it is now conceivable to apply rational structural design principles to earthen construction for the first time in history in the late twentieth century. Regarding the seismic, thermal, and moisture durability performance of earthen structures. Some of those standards are: (ASTM 2010).

- Australian Earth Building Handbook
- California Historical Building Code
- Chinese Building Standards
- Ecuadorian Earthen Building Standards
- German Earthen Building Standards
- Indian Earthen Building Standards **(IS 13827:1993)**
- International Building Code / provisions for adobe construction **(IBC ,2019)**
- New Mexico Earthen Building Materials Code (NM, **Commission of Public Records 2008a)**
- New Zealand Earthen Building Standards (**NZS 4298b ,1998b) d**
- Peruvian Earthen Building Standards

When dealing with natural risks and other disasters such as earthquakes, earthen construction should be technically developed. According to a comparison study carried out by (Tayyibi, et al. 2016), none of the codes or laws addressed all types of earth construction technical solutions or security regulations. Above all, there are limited codes and guidelines for un-stabilized adobes, which focus on the construction methods rather than on the properties of the constituent materials.

Code developed to the date mentioned less about the cause of the failures and (almost all literature) turned a blind eye to the seismic survival of earthen buildings while pointing critically to those that failed. Some of the code developed around the world regarding the adobe is shown in Table 2-12**.**

Table 2-12 some of the code developed around the world and their comments on specified topics

	Description	(IBC 2019)	NM	ARIZ	NZS	IS 13827:1993	Peruvian code	ASTM
1	**Earthen material requirements** Composition of the earthen adobe block	For stabilised adobe only	limits on warping or cracking *qualified soil <2% soluble salt	In conformance with (UBC) Standard 71-1 Sufficient clay, Contains no or <2% soluble salt		"suitable soil"	10–20% clay, 15–25% silt, 55–70% sand, no organic soils, may contain straw, no stones > 5 mm.	General (no specific description)
2	**Construction Methods**							
	mortar	Same as adobe soil	same as earth blocks,or lime cement	same as earth blocks	reference to **NZ98**	Same as the block(+straw /sandsometimes)	Soil+stabilizer or Soil +straw	(no comment)
	Un stabilized exterior earthen walls finishing	requires two-coat cement plaster	earth plaster cement plaster	Cement plaster	Defined and detailed process of plastering and curing	Mud plaster, cow dur and stabilizers like bitumen ,kerosine	sand-cement mortar with wire mesh	Cement plaster
3	**Physical properties**							
	The dimension [mm] (recomended)					380x250x110 380x380x110		
4	**Limit of story**	Not exceed one,Two if designed by professional.	One and two story	One story	walls up to 6.5 meters high	One and two story	One and two story	Not mentioned
5	**Mechanical Properties [kPa]**							
	a minimum average compressive strength	2068 >1724 (not less than)	2068	2068		1200	200	
	Ultimate compression	2,000	2,000	2,000	1,300	1200	1200	
	Modulus of rupture	340	340	380	250			
	Allowable compression	200	200	200			200	
5	**Testing and quality control**	A vertical load shall be applied to the cylinder at the rate of (37 N/s) until failure occurs.	requires sample compression tests	(no comment)	requires and defines curing for cement and lime-stabilized earth;	field tests (for desired properties)defined and illustrated	field tests(for allowable stresses) defined and illustrated	general reference to tests for similar materials

*Qualified soil means any soil, or mixture of soils, that attains 300 psi compression strength and attains 50 psi. Modulus of rupture.

2.8 Adobe failures and its enhancing mechanisms /damage associated to adobe

Adobe failures are mostly associated with poor design and material properties not being studied to a higher level. Adobe faces natural and man-made disasters as the other material experiences.

2.8.1 Seismic failure

It is a failure caused by an earthquake force that deteriorates the adobe structure following the weak zone, as shown in figure 2.13. and Figure 2.14.

This failure can be improved by experimenting with different mechanisms, like reinforcing the structure and determining the appropriate mix ratio. To increase the seismic performance of earthen buildings initially, one needs to know its failure mechanisms too.

Then, using cost-effective methods which ensure seismic safety will be addressed for the large section of the world's population. Meli et al. 1980, conducted a series of shake-table tests using 1:2.5-scale adobe buildings almost four decades ago, marking the beginning of research with that focus.

Table 2.13 shows some of the earthquake damages on adobe building in different parts of the world even though the survivals are kept surreptitious.

Table 2-13 Earthquake damage on adobe building

EQ name	Fatalities	Damage on Adobe building	Structural failures	Refrence
Peru/1970	40,000	on rocky terrain,damage,was minimal,	many adobe buildings withstood the effect of the earthquake and are still inhabited.	(P.Doat, 1991)
El Salvador /2001 Mw 7.7,	1,100	200 000 adobe houses were severely damaged or collapsed	Total collapse	Dowling [2004] Dowling [2004a]
South of Peru	81	attributed to the 25,000 adobe houses that collapsed and the 36,000 that were damaged		(USAID Peru 2001)
Northridge /1994 (Mw 6.7)	60	damage survey on 20 historic and 9 older adobe buildings in California is observed.		(Memari and Kauffman ,2005)
Bam ,Iran /2003	more than 43,000	over 60,000 were left without shelter	Parapet collapse on an adobe building	(EERI 2004) (source: Mehrain and Naeim 2004)
Pisco, Peru/2007	More than 600	destroyed more than 75,000 dwellings.	Out-of-plane wall collapse Roof collapse on an adobe building	(INEI 2007)

2.8.2 Types of seismic failure

Researches showed that Adobe is a low-strength building material, and the walls of adobe buildings are thick and massive. So, the stresses in the adobe masonry during an earthquake can easily exceed the tensile strength of the material, and cracks will develop.

Figure 2-13 In-plane failure.

Figure 2-14**.** Out-of-plane failure**.**

In -plane shear cracks

Diagonal cracks are typical results of in-plane shear forces which act horizontally in the plane of the wall. This force causes tensile stresses approximately at 45 degrees to the horizontal.

Out of plane damage

The extent of damage is often not particularly severe as long as the wall is prevented from overturning.

2.9 Modeling of adobe building

Building the prototype needs high investment in the material to be tested, equipment for the testing, and workforce for the process of construction and testing. So it is vital to develop a means of evaluating the properties and capabilities of the structure with minimum investments in capital and with a minimum error that can be achieved by utilizing the reduced-scale modeling of the prototype or simulation analysis.

As per the explanation of (Harris and Sabnis 1999) model analysis has limitations. The fundamental benefit of a physical model over an analytical model is that it describes the behavior of a fully-loaded structure up to the point of collapse. Despite significant advances in computer-based approaches for structural analysis, we still cannot forecast the failure capacity of many three-dimensional structural systems analytically, especially under complex loadings. Because the concentrated load on a prototype is lowered in proportion to the square of the geometric scale factor of the model (a 100-kN prototype load is 0.25 kN on a 1/20-scale model), the load-reduction factor is the most striking shown for different model scaling parameters in Table 2-14 which derived from similitude and dimensional analysis theory.

The scaling law for static elastic modelling can be shown as, (Al.Vasilescu 1969) cited in (Monica Nicoreac et al 2010):

$$S_\sigma = \frac{S_F}{{S_L}^2}\ ;\ S_\delta = \frac{S_F}{S_L S_E}\ :\ S_\sigma = \frac{S_F}{{S_L}^2}\ :\quad S_\gamma = \frac{S_F}{{S_L}^3}\ ::\quad S_\tau = S_G \frac{S_F}{{S_L}^3}\ ;\quad S_\mu = 1$$

Table 2-14 Similitude requirements for static elastic modeling

Material Properties	Dim.	Scale Factors	Geometry	Dim.	Scale Factors	Loading	Dim.	Scale Factors
Stress σ	FL^{-2}	S_E	Linear dimension l	L	S_L	Concentrated load Q	F	$S_E S_L^2$
Modulus of elasticity E	FL^{-2}	S_E	Linear displacement δ	L	S_L	Unif. distrib. load w	FL^{-1}	$S_E S_L$
Poisson's ratio μ	-	1	Angular displacemnt	-	1	Pressure/surface load q	FL^{-2}	S_E
Specific Weight γ	FL^{-3}	S_E/S_L	Area A	L^2	S_L^2	Moment M or torque T	FL	$S_E S_L^3$
Strain ε	-	1	Moment of inertia I	L^4	S_L^2	Shear force V	F	$S_E S_L^2$

Similitude requirements for static elastic modeling can also be putted in another form like Table 2-14, (Harris and Sabnis 1999) . We can see that the stresses on the prototype are SE times larger than those on the model, while the strain on both model and prototype are the same. The loadings on the model are scaled by a large factor $S_E\ {S_L}^2$.

The most significant drawbacks of employing structural models in a design context are time and cost. When comparing physical models to analytical models, it is clear that the latter is usually less expensive and faster, and physical models cannot be expected to supplant or replace analytical modeling of structures when the analytical modeling procedure results in an acceptable - definition of prototype structure behavior. As a result, physical models are virtually always limited to circumstances where mathematical analysis is insufficient or impossible. Another stumbling block is that changes in the prototype design as a result of a model study may necessitate the use of a second model to double-check the design. As a result of practical considerations, the model is frequently used to verify a "nearly finalized" design (Harris and Sabnis 1999).

2.10 Choice of geometric scale

Geometrical scaling is categorized into subsections Specimen and modeling scales. Determining the specimen scaling from model to prototype is critical to do earthquake resilience analysis. In addition, the model scaling factor from model to prototype adobe walls is used to determine cracks.

2.10.1 Model and Prototype Similarity Analysis

To figure out which qualities are the best under future operating conditions models, are subject to various tests, including the similarity method which, entails scaling the results of a model-based experiment to the full scale of the actual prototype. The model we want to utilize to figure out what attributes the prototype should have been similar to the prototype. If all dimensionless parameters have equivalent values, this similarity is ensured.

There are three forms of mechanical system similarities, as well as one type of thermal system similarity: which are **Geometric, Kinematic, Dynamic, Thermal similarity**, respectively (Jazar 2020)**.**

Model and prototype have the same ratio of all related lengths; hence the model is a smaller or enlarged copy of the original.

2.10.2 Shapes of buildings in the model and the prototypes

A structural model is defined as "any physical representation of a structure or a portion of a structure. Most commonly, the model will be constructed at a reduced scale." This definition has been evolved by ACI Committee 444.

3 METHODOLOGY

3.1 Introduction

This research is a basic type of research that has been conducted to develop knowledge, theories, and predictions by applying primary and secondary data collected.

3.1.1 Importance of the methodology

The importance of the methodology was achieved following the methodology

- To formulate the problem and objective mentioned and present the result from the data obtained during the study.
- To test the performance of adobe in a controlled conditions before bringing it to actual construction industry through experimental research.

3.1.2 Research question

The question of this research is:

- What is the relationship of roof load and earthquake forces.?
- How can we calculate the seismic performance of the circular adobe structure?
- What is the failure angle from the static tilt tests which indicate the ultimate horizontal force for each model and the Percentage of horizontal force compared model own weight whatever earthquake testing mechanism used?
- What is the typical failure pattern of the circular adobe structures?

3.1.3 Research Aim

The aim of this research is to enhance the performance of adobe building which initiate its preferability to modern architecture which are just sustainable and eco-efficient dwellings.

To provide reliable design guidelines for different builder and practicing engineers on structural capacity of earthen adobe block and members.

3.2 Research design

Maximizing the earthquake resistance of circular adobe building designed a research technique and chosen, as it points out how relevant information for a study will be acquired.

3.2.1 Philosophy of the research design

It was just to determine the failure and enhancing (tackling the failure) mechanism of the cheap, abundant and environmentally friendly earthen martial to useful cheap, simple and engineered building structure by applying simple static tilt table test to measure the capacity to earthquake disaster.

3.2.2 Types of research method

Experimental research approach with a quantitative data collection and analysis method was used.

3.2.3 Research Strategies

The approach of this thesis was quantitative, from the data collection to analysis and result formulation.

3.2.4 Data collection of the adobe constituent materials

Quantitative primary data collection with non-probable sampling (the raw soil and teff straw (chid) sample has been taken purposely from its past reputation as a building material). The straw as a binding stabilizing element also directly selected from the traditional technique of mud preparation to reduce the cost of number of probable samplings.

3.2.5 Determining Adobe making Materials

In general, the primary steps in the production of earth (adobe)block are selecting the constituent materials like the soil, straw and so on in the field and laboratory.

3.2.5.1 Determining composition of the constitute materials of the soil

Certain soil types appear to yield strong adobe building than others. This shows that the percentage composition of the soil also matters.

So, it is better to investigate the locally familiar and available soil, which has been taken by non-probable sampling, before undergoing further tests.

3.2.5.2 laboratory test to determine composition of the soil

The process of gradation of the soil particles was analyzed using Sieving method (dry soil using sieving machine) and hydrometer tests in the laboratory.

Soil particles above 0.075 mm were sieved. The percentage of soils passed 0.075mm sieve, which are the clay and the silt, was also determined with a hydrometer test. 'Good adobe soils contain only a small amount of gravel particles.' (Clifton 1977)

Based on the standard classification of soil by the USCS, particles in the range of 2 to 0.02 mm are sand, particles in the range of 0.02 to 0.002 mm are silt, and particles smaller than 0.002 mm are clay.

a) Sieving the dry soil and determine percentage retained

i) Had taken a 2 kg sample of soil, washed it in a pail container, sieved it through 0.075 mm (#200) sieves, dried it in the oven, and weighed the retained material that is > 0.075 mm in size (Kitch 2009).

ii.) had sieved the dried sample with a vibrating machine and weighed the soil retained on different sizes of sieves.

iii) tabulated the particle size distribution, sieve analysis, and drew the curve of particle size versus percentage passing.

b) Hydrometer test

steps to follow are

i. Compute the moisture content (in percent)

$$W = \frac{M_w}{M_s} \text{ x } 100\% \qquad \ldots\ldots\ldots\ldots\ldots \quad 3\text{-}1$$

Where: W = moisture content (in percent)

Mw= mass of the water in the soil sample

Ms = mass of the soil solids in the soil sample

ii. Compute the dry mass of the slurry in the hydrometer.

$$M_d = \frac{M_3}{1+W} \qquad \ldots\ldots\ldots\ldots\ldots \quad \mathbf{3\text{-}2}$$

Where: M_3 =total mass of soil in the hydrometer slurry

W =moisture content of soil in decimal form

iii. Compute the equivalent dry total sample mass, Me

$$M_e = \frac{M_d}{P_{-\#10}}.100\% \ \ldots\ldots\ldots\ldots\ldots\ldots\ldots \ 3\text{-}3$$

, Where $P_{-\#10}$ =percentage passing #10 sieve (from the sieve analysis)

iv. Determine the *Specific Gravity of the soil (G_s) in the labratory*

v. Compute the particle diameter, D, for each reading

$$D = \sqrt{\frac{30\eta}{981(G_s - 1)\rho_w}\frac{L}{t}} \ldots\ldots\ldots\ldots\ldots\ldots \ 3\text{-}4$$

Where:
D= particle diameter (mm)

η =dynamic viscosity of water (in poise)

L=effective depth (in cm)

G_s=Specific gravity of soil solids

ρ_w=density of water=1gm/cm^3

t= elapsed time since beginning of test (min)

iv. Specific Gravity of the soil G was determined using pycnometer

V. The particle distribution was determined and classified the soil composition.

Percentage of Gravel, Sand and silt has been determined in the raw soil.

3.2.5.3 Field soil properties tests for Adobe making criterion

To avoid being too clayey, which easily cracks, and too sandy, which cannot be bonded together, the mud mix without the straw undergone field soil properties test and those which have passed this criterion will be mixed with the straw for the adobe production.

a) During the on-site inspection, sensory test (smell test) was performed to detect the presence of organic matter and to assess grading (touch test).

b) A dry strength test was done to check the plasticity of the soil. The mud ball was difficult to crush if it had adequate fines for mud brick.

c) The ribbon test was used to determine the relative grading of soil and its suitability for mud brick, with the ribbon length ideally falling between 60 and 120 mm (Walker 2002).

d) Field soil composition test (Sedimentation Test)

Prior to production of the adobe the composition of the soil in the field is tested to make sure that the sample taken matches with the soil tested in the laboratory for specimen production and testing.

3.2.6 Production of the adobe

It is a procedure in which graded soil, teff straw (chid), and water are mixed, moulded, and dried.Taking the data from the hydrometer test as an initial parameter of the soil properties, the mud that had been prepared and poured into the moulds had dried in the sun and shaded for three to four weeks, not less.

a) Prepare different trial mixture of soil and straw

The trial mud, from which the representative of the adobe for the prism test was to be prepared, contained different proportions of sand, silt, and clay that passed the criterion of the field test.

c) Production and drying of the adobe block

Arranged the appropriate size mould for the production of the specified trial mix design, then poured the mud into the mould and dried it for a minimum of 28 days, of which four days in the sun and the rest in the shade. (Blondet and Vargas 1978)

3.2.7 Adobe block compression masonry prisms test

According to ACI 530.1-11/SCEA there are two types of compression tests for masonry;

Unit strength and prism test method

i) Unit strength Method

It is a compression test on adobe cubes. For the case of adobe units as per the recommendation of (Blondet and Vargas 1978) different nominal dimensions were fabricated for axial compression test.

ii) Prism test method

It is compression tests on adobe prisms according to Standard test method for compressive strength of masonry prisms (ASTM 2014). The aspect ratio factor has been used from the Australia Standard AS 3700-2001 (Standards.Australia 2001) just for the sake of comparison with the previous research.

The compression prism specimen was prepared and tested following the steps

- cutted the full-size adobe into two pieces measuring 200X150X100mm each.
- Constructed a three-quarter adobe prism
- The compression prism had been dried.
- Delivered the compression prism to the testing laboratory
- The compression prism had been capped.

Besides the compressive strength of the adobe prism, modulus of elasticity (E) of the adobe prisms was determined by using the stress-strain data from the compression test by installing LVDTs to capture deformation measurements of the triplet prisms.

3.3 Modeling process

By utilizing strength modeling to predict prototype behavior for all loads up to failure.

1. determined the problem's scope (by determining what was required and what was not from the model).
2. Specified similitude requirements for geometry, materials, loading, and result interpretation if necessary.
3. Decided on the size of the model and the required level of reliability or accuracy. What size model should be used to be consistent with the accuracy? (Took the same model size of the previous research for the sake of comparison).
4. Selected model materials, paying close attention to steps 1–3 above.
5. planned the fabrication phase, and model building activities closely.
6. selected strains, displacements, forces, and other quantities measuring equipment and instruments.
7. Designed and prepared loading equipment if there is so; in this case manual increasing loading was used.
8. Observed the response of the model during loading, taking complete notes and photographic records of the behavior. There were five video recorders in this phase to record detailed comments on load history, cracking development, instability modes, and other information that may be difficult to describe numerically.
9. Analyze the data and write the report as soon as possible, while the entire test is still fresh in your mind. In addition to reporting the results, suggestions for improvement in techniques should be recorded to facilitate better modeling results in subsequent experiments (Harris and Sabnis 1999).

3.4 Tilting Table Test

Prior to testing of the model, the static tilt table is designed, assembled and checked for its loading capacity.

3.4.1 Analysis and Design of the testing table load bearing members

The plane dimension of tilt table is 1.5 m by 1.5 m and having a maximum capacity of 2.5 ton which is driven by electric with hydraulic pump to make the lifting pressure constant without disturbance. Digital angle finder (goniometer) is attached to measure the tilting angle ,θ ,of the loaded model from zero to the maximum where the first crack and complete collapse occur.

Method of calculation for the Tilt table parts

- Hand calculation
- Finite element modeling analysis and design using ETABS 17

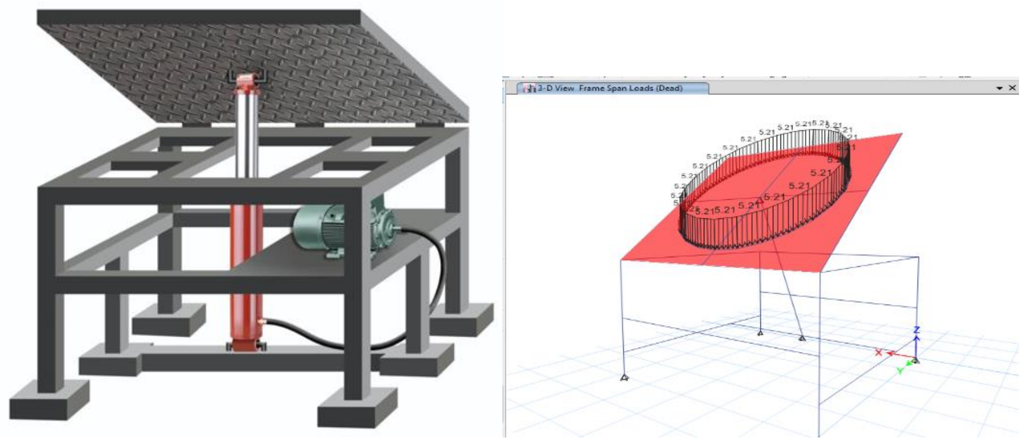

Figure 3-1 Design of static tilt table using FE soft. ETABS 17

3.4.2 Static tilt table testing

To perform the test, with analytical modeling needs so many parameters (properties of the adobe which is not clearly defined yet) which is not as such accurate. So, the Static Tilt Table Test (STTT), which is validated with that of the pushover test (see section2.5.1), makes it useful to evaluate the seismic performance of circular adobe buildings. The adobe house models, when tilted up on a static tilt table, will be subjected to a constant acceleration (due to gravity load, its own weight, and roof load). The structure will be studied during tilting up until failure to predict what should happen to the structure in a real earthquake, as explained in section 3.4.3.

Figure 3-2 Modified static tilt table

3.4.3 The simulation of the result with the earthquake magnitude

The angle of the static tilt table at which the first cracking appears is used to calculate the maximum lateral force, which adds vital information that benefits both researchers and practicing engineers.

Pseudo static analysis

Method of analyzing the slope subjected to earthquake force.

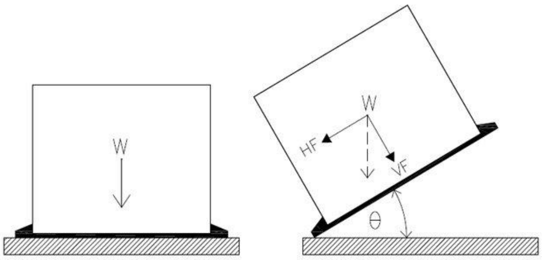

Figure 3-3 Concept scheme of the static testing.

Number of variables*:* *As* figure 3.3 shows the weight of the model (W) transforming to lateral force (HF) which is equivalent to horizontal inertial force obtained by the acceleration (a_h). a_h has been generated by the Earthquake shaking in pseudo static analysis when tilted at angle θ (the failure angle). W, HF and a_h.

$$H_F = \mathbf{a_h} * M * \frac{\mathbf{g}}{\mathbf{g}} = W * \text{Sin}(\theta) \ldots\ldots\ldots\ldots\ldots\ldots\ldots\ldots\ldots \quad 3\text{-}5$$

$$H_v = \mathbf{a_v} * M * \frac{\mathbf{g}}{\mathbf{g}} = \frac{a_v}{g} * W \quad \ldots\ldots\ldots\ldots\ldots\ldots\ldots\ldots \quad 3\text{-}6$$

Where: **Hv** is the vertical inertial force which alters the weight which alters the base normal which in turn alters the base shear resistance, $\boldsymbol{H_F}$ is the horizontal inertial seismic force which have a dramatic effect on the stability of a slope, and $\mathbf{a_h}$ and $\mathbf{a_v}$ are the horizontal and vertical Pseudo static acceleration respectively.

K=a/g = dimensionless coefficient of acceleration ………… 3-7

Therefore, the inertial effect is specified as

$$\mathbf{K_h} = \frac{\mathbf{a_h}}{\mathbf{g}} = \boldsymbol{Sin(\theta)}, \textbf{ and } \mathbf{K_v} = \frac{\mathbf{a_v}}{\mathbf{g}} = \boldsymbol{Cos(\theta,)} \ldots\ldots\ldots\ldots\ldots\ldots \text{3-8}$$

Where: K_h and K_v are the coefficient of acceleration in horizontal and vertical.

Earthquake force is dynamic but it is possible to consider the inertial force as the major element responsible for instability.

Assumption: - inertial force is static which is acceptable for moderate level earthquake.

In pseudo static approach the acceleration generated by earthquake shaking is considered to create inertial forces and directions. As the seismic coefficient increase (K_h) there should be smooth gradual decrease in the safety factor.

"A serious earthquake (0.35 g) has the same effect on a house as tilting it at an angle of 20.5 degrees. That's why walls must be strong" (SADC 2006).

K=0.35, $\mathbf{a_h}$=g sin(θ) =0.35 g, which gives $\theta=\sin^{-1}(\frac{a_h}{g}=K)= \sin^{-1}(0.35)=20.487$ degree

So, a model tilted at an angle of θ=20.5 Deg. is equivalent with experiencing an earthquake with a seismic coefficient of acceleration K=0.35.

The hazard is described by the reference peak ground acceleration (PGA) on type of ground, a_{gr}=a , (PGA)= K=G=coefficient of acceleration= a_o/g

Number of tests

A small-scale circular model (1:3 scale) adobe structures was built and tested with the configurations and roof loads taken from the previous research maximum output (Jinwuth 2012).

Here the number of tests was limited to one since it is time taking, relatively expensive and less possibility of error occurrence.

3.4.4 Data analysis software

The ETABS software compared and analyzed the outcomes of variables utilized in the design of the static tilt table. Excel is also used to create the illustrations and calculate some of the analytical solutions tables and graphs.

3.4.5 Reliability of data analysis

The analysis of gradation is reliable since it was standard method of testing besides the result of the laboratory against the field test were the same.

As per the previous research done described in chapter 2 section 2.5.1 of this thesis the data obtained and analyzed from the static tilt table is reliable since it was validated with the pushover test.

4 RESULT AND DISCUSSION

4.1 Gradation of the constituent Soil

According to the method described in chapter three, the soil taken from the non-probability sampling method was tested and classified in the laboratory.

The step used in the classification was described in section 3.2.5, a sieve analysis and hydrometer test were used to determine the proportions of the gravel, sand, silt, and clay in the soil.

The sieve analysis should always generate results for grain sizes smaller than 0.1 mm. In general, silt particles range from 0.075 to 0.002 mm. Clay particles are smaller than 0.002 mm.

In the laboratory, sieve and hydrometer analysis, which followed step-by-step methodology, is reported.

4.1.1 Classification of the soil

From the analysis of the laboratory tests, the result shows the composition of the soil chosen for the production of adobe was 7.46% gravel, 54.43% sand, and 38.11% silt and clay, which can be classified as silt (SM) and silty soil (A4) according to Unified and ASTM D3282 classification respectively.

In the field, a sieve of no. 4 (4.75mm) has been used to screen out the particles larger than 4.75mm, so that the granular materials (4.75%) had been replaced by sand, silt and clay proportionally which yield 58.817% sand and 41.17% silt and clay. The proportion on-site with sedimentation test after screening the granular has proved it, see figure 4-1.

To change the soil property to that of the previous research, i.e., 85%, of sand and 15%, silt and clay from a sedimentation test., must have to blend 0.636m^3 of sand to 0.364m^3 of raw soil.

i.e. Ratio of Raw soil to sand to be blended = RS: S =1:1.745

Where: RS and S stands for raw soil and Sand blended respectively.

Sieve Analysis

Project Title: Gradation of Soil for Adobe production ***Test performed by: Habtamu H. Michael***

Test Date: December 17, 2019 ***Checked by:***

USCS Soil Classification: Silty Sand (SM), , Dry

Moisture Content of the soil tested

Moisture Can ID Number	177	3	R114	
Mass of tin	15.4	13.79	15.89	**gm**
Mass of wet soil and tin	29.05	27.44	26.1	**gm**
Mass of dry soil and tin	26.87	25.13	24.56	**gm**
Moisture Content	19	20	18	**%**
Average Moisture Content	19			**%**

Sample mass before wet washing

Mass of bowl	494.4	**gm**
Mass of sample and bowl	2494.4	**gm**
Mass of Sample	2000	**gm**
Total dry mass of sample (weight of solids)	2000	**gm**

Sample mass after wet washing

Mass of evaporating dish	494.4	**gm**
Dry mass of sample greater than#200 sieve plus evaporating dish	1,732.2	**gm**
Dry mass of sample greater than#200 sieve	1237.8	**gm**
Dry mass of sample less than#200 sieve (portion washed out)	762.2	**gm**

Sieve analysis

Sieve Number (in)	**Diameter (mm)**	**Mass of Empty Sieve (g)**	**Mass of Sieve & Soil (g)**	**Soil Retained (g)**	**Soil Retained (%)**	**Cumulative percent retained**	**Percent Passing**
1	**25**	1213.30	1245.90	32.60	1.63	1.63	98.37
3/4	19	1118.70	1118.70	0.00	0.00	1.63	98.37
1/2	12.5	1181.40	1212.80	31.40	1.57	3.20	96.80
1 1/2	9.5	1157.40	1184.40	27.00	1.35	4.55	95.45
4	4.75	1262.4	1320.6	58.20	2.91	7.46	92.54
8	2.36	983.3	1098.8	115.50	5.78	13.24	86.77
10	2	943.9	989.3	45.40	2.27	15.51	84.50
16	1.18	895.2	1037.2	142.00	7.10	22.61	77.40
30	0.6	830.3	1093.7	263.40	13.17	35.78	64.23
50	0.3	752.4	1041.9	289.50	14.48	50.25	49.75
100	0.15	780.2	925.1	144.90	7.25	57.50	42.51
200	0.075	733.5	821.4	87.90	4.40	61.89	38.11
Pan		765.60	1527.80	762.20	38.11		
			TOTAL:	**2000.0**	**100.0**	7.46	gravel
						54.43	sand

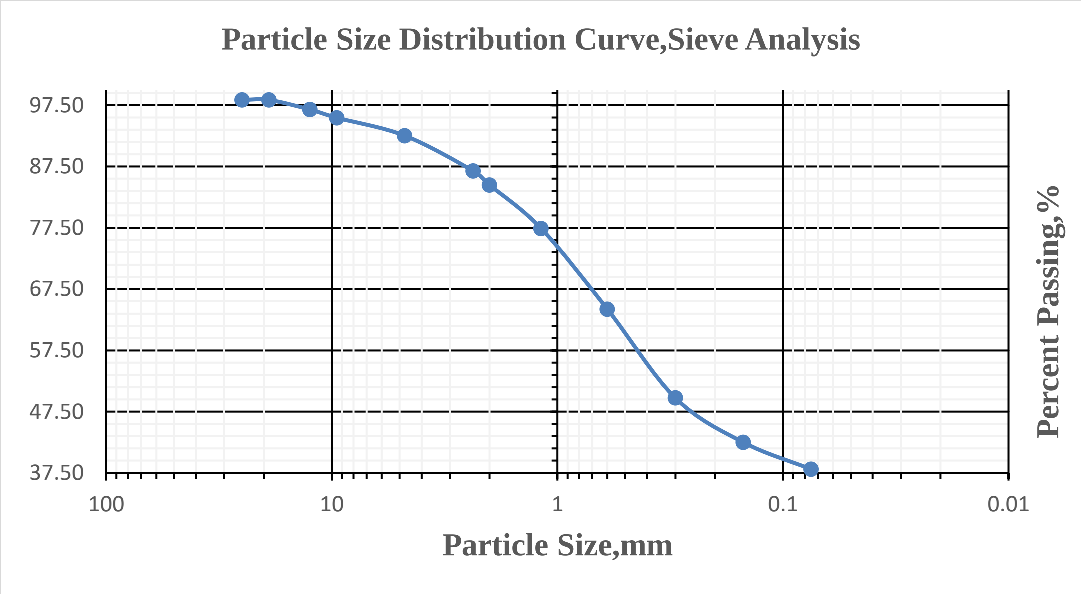
Particle Size Distribution Curve,Sieve Analysis
97.50
87.50
77.50
67.50
57.50
47.50
37.50
100
10
1
0.1
0.01
Particle Size,mm
Percent Passing,%

Hydrometer Analysis

Project Title: selecting Soil for Adobe production ***Test performed by: Habtamu H. Michael***

Test Date: ***Checked by:***

USCS Soil Classification:

Moisture Content of the soil tested

Moisture Can ID Number	**177**	**3**	**R114**	
Mass of tin	**15.4**	**13.79**	**15.89**	**gm**
Mass of wet soil and tin	**29.05**	**27.44**	**26.1**	**gm**
Mass of dry soil and tin	**26.87**	**25.13**	**24.56**	**gm**
Moisture Content	**19**	**20**	**18**	**%**
Average Moisture Content		**19**		**%**

Specific Gravity of the soil Gs

Correction factors	K	
Determination Number	1	2
Temprature ,Tx	17	21.2
Density of water	0.99880	0.99802
K	1.00060	0.99980

Specific Gravity for Sampled Natural Soil				
Calibration of Pycnometer				
Mass of dry,Clean Pycnometer, Mp,g	63.9	Density of water		
Mass Pycnometer + Water, Ma,g	163			
Observed Temprature of water,Ta	17	0.99880	Mass of can	45
Specific Gravity Determination			Can+D.soil	73.8
Determination Number	1		Mass of Soil	28.8
Mass of dry,Clean Pycnometer, Mp,g	63.9			
Mass of Pycnometer + Specimen, Mps,g	92.7			
Mass of Pycnometer +Soil+ Water, Mpsw,g	180.8			
Temprature Contents of pycnometer when Mpsw was taken,Tx,g	17			
Mass Pycnometer + Water at Temprature,Tx Ma,g	162.98			
K for Tx	1.00060			
Specific Gravity at measurd temprature	2.6222			
Specific Gravity at 20°c=K*Gs at Tx	2.62378			
Average Specific Gravity at 20°c	2.62			

Specific Gravity for Sampled Natural Soil				
Calibration of Pycnometer				
Mass of dry,Clean Pycnometer, Mp,g	**58**	**Density of water**	**Mass of can**	**51.7**
Mass Pycnometer + Water, Ma,g	**158.6**		**Can+D.soil**	**80.8**
Observed Temprature of water,Ta	**21.2**	**0.99802**	**Mass of Soil**	**29.1**
Specific Gravity Determination				
Determination Number	**2**			
Mass of dry,Clean Pycnometer, Mp,g	**58**			
Mass of Pycnometer + Specimen, Mps,g	**87.1**			
Mass of Pycnometer +Soil+ Water, Mpsw,g	**176.5**			
Temprature Contents of pycnometer when Mpsw was taken,Tx,g	**21.2**			
Mass Pycnometer + Water at Temprature,Tx Ma,g	**158.60**			
K for Tx	**0.99980**			
Specific Gravity at measurd temprature	**2.59821**			
Specific Gravity at 20°c=K*Gs at Tx	**2.59769**			
Average Specific Gravity at 20°c	**2.60**			

$$Gs=\frac{2.62+2.60}{2}=2.61$$

Hydrometer Sample Data

Mass of beaker	**tared**	**gm**
Mass of sample and beaker		**gm**
Mass of Sample,M3	**50**	**gm**
Total Dry Mass of Sample (weight of solids), Md	**42.0168**	**gm**
Equivalent Dry Mass of Total Sample, Me	**49.7270**	**gm**

Time (T) (min)	**Temp (°C)**	**Hydrometer Reading in Test cylinder, Ra**	**Effective L(cm) Table 2,D422**	**Dynamic Viscosity ofwater(poise)**	**Particle Diameter, D(mm)**	**Hydrometer Reading in control cylinder,r**	Percent finer,% (by D422)	Adjusted Percent Finer
0.75	17.5	1.0315	7.95	0.010740	0.0465183	1.002	96.20	36.66
1	17.5	1.0305	8.25	0.010740	0.0410391	1.002	92.94	35.42
2	17.5	1.0285	8.75	0.010740	0.0298855	1.002	86.41	32.93
4	17.5	1.0245	9.85	0.010740	0.0224212	1.002	73.37	27.96
8	17.5	1.022	10.5	0.010740	0.0163689	1.002	65.22	24.85
15	17	1.021	10.7	0.010880	0.0121459	1.002	61.96	23.61
30	16.5	1.0195	11.15	0.011020	0.0088234	1.002	57.07	21.75
60	16.5	1.0183	11.44	0.011020	0.0063197	1.002	53.15	20.26
120	17	1.0172	11.74	0.010880	0.0044981	1.0015	51.20	19.51
240	17	1.0162	12.04	0.010880	0.003221	1.0012	48.91	18.64
480	19	1.015	12.3	0.010340	0.0022442	1.0012	45.00	17.15
960	14	1.01463	12.412	0.011750	0.0016993	1.0012	43.78	16.68
1440	15.5	1.01425	12.525	0.011305	0.0013671	1.0012	42.56	16.22

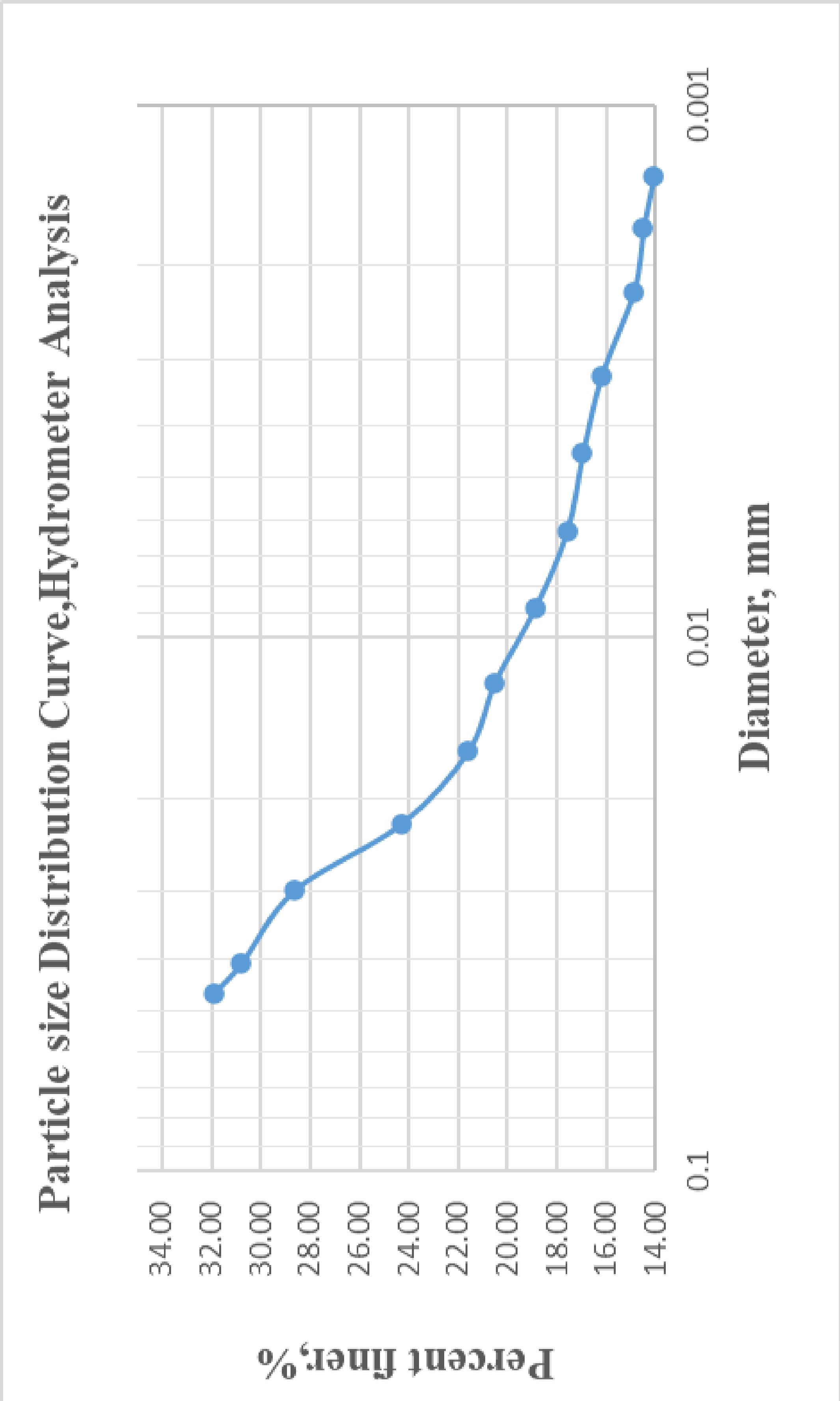
Particle size Distribution Curve,Hydrometer Analysis
Percent finer,%
34.00
32.00
30.00
28.00
26.00
24.00
22.00
20.00
18.00
16.00
14.00
0.1
0.01
0.001
Diameter, mm

4.2. Adobe production

4.2.1 Adobe making Materials and their Relevant Tests

Not all soil is suitable for adobe construction. Ideally the soil should be made up of:

- sand:55 -75%
- clay: 15 - 18%
- Silt: 10 - 28%
- Organic materials <3%

According to builders who used to use this technique “red, non-organic earth, not too wet, should be chosen and building work should take place preferably in the Spring, when the sap is rising in the soil.” (Doat, et al. 1991).

4.2.2 Field soil Property test for Adobe making criterion

So as to confirm the laboratory tested soil same with the field soil to be used for the production simple field test has been done while mixing the soil.

a) Sedimentation Test

Sedimentation Test is a soil composition testing mechanism, In a glass jar, the mixture is mixed with a lot of water. The larger particles sink to the bottom, while the finest particles rise to the top. Many sources (e.g., CRATerre, 1979; International Labour Office, 1987; Houben, Guillaud, 1984; Stulz, Mukerji, 1988; United Nations Centre for Human Settlements) state that the height of each layer correlates to the proportion of clay, silt, sand, and gravel, but this is incorrect.

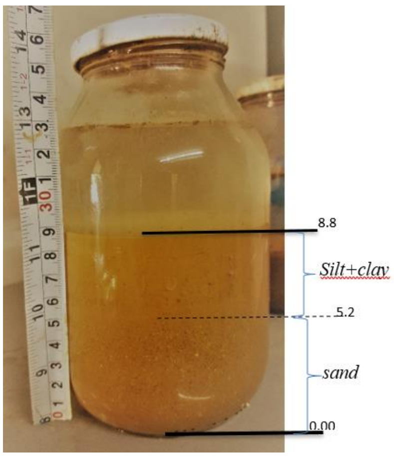

Figure 4-1 Field soil sedimentation test

Here we see that clay and silt and the sand boundary horizon about 5.2cm height of the glass which indicates that 5.2/8.8*100=59.09% of sand.

The result of the sedimentation test in the field (production site) shown in figure 4-1. Was the same as the laboratory values (58.817% of sand and 41.17 % of Clay and silt) excluding the coarse aggregate by sieving.

b) Sensory testing undertaken during on-site inspection for the presence of organic matter (smell test) and to assess grading (touch test).

c) A dry strength test was made to check the plasticity of the soil, so it was hard to crush the mud ball if it had adequate fines for mud brick.

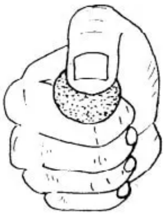

Figure 4-2 dry strength test

d) The ribbon test was used to determine the relative grading of soil and its suitability for mud brick, where the ribbon length should be between 60 mm and 120 mm. see Figure 4.2. (Walker 2002).

Figure 4-3 Ribbon test (for the trials).

4.3 Trial mix for the adobe production

Had mixed raw soil (58.82 % sand, 41.18 %t clay, teff straw (chid), and some blended with sand) with proportional water, and let it soak for more than a week by adding some water, mixing it once every three days to break the coarser soil particles. Figure 4-3. shows trial-mixed mud that has passed a field test.

Six trial mix compositions have been made, and five of them have passed the field test for further adobe production to the compression test (Table 4-1).

Figure 4-4 mud composed of sand silt clay and straw

4.4 Production of the adobe specimen

Before productionn of model adobe for the static tilt table test (STTT) from different composition trial mix which passed the field test described in section 4.2.2 and Table 4.1 adobes were produced to determine the peak compressive strength mix design .

The trial mix composition, which passed the field criterion test, was used to produce the representative adobe prism as follows.

In the previous research, a mould of an approved size was used. According to the ASTM 1314-14 standard, L = 30, W = 20, and H = 10 cm.

Table 4 1 trial mix proportion result of field criterion test and number of sample adobe

	Mix ratio by volume			Field Tests (for the raw soil and sand blending)			Adobe Produced For prism test	Quantity Of adobe block produced
Trial	**Raw soil**	**sand**	**teff straw "chid'**	**Sensory testing**	**Dry strength test**	**Ribbon test**		
1	**2.73**	**1.29**	**1**	**Passed**	**Passed**	**Passed**	**A**	**8**
2*	**2**	**2**	**1**	**Passed**	**Failed**	**Failed**		**none**
3	**2**	**1**	**2**	**Passed**	**Passed**	**Passed**	**B**	**12**
4	**3**	**1**	**2.5**	**Passed**	**Passed**	**Passed**	**C**	**8**
5	**2**	**0**	**1**	**Passed**	**Passed**	**Passed**	**D**	**8**
6	**2**	**1**	**1**	**Passed**	**Passed**	**Passed**	**E**	**8**

2* the composition of the raw soil is blended with sand to 85% sand and 15 % silt and clay

Wet the internal part of the mould with water to ease the removal of the cast mud within minutes..

- Because the mould's base was open and would be used frequently, arrange the receiving base as shown in figures 4-4a and c, preferably with burnt oil polished.
- Poured the mud into the mold and gently pressed down to distribute it evenly and reduce the void.
- Liftted the mould up using the provided handles, as shown in figure 4-4-c.
- Dried it with direct sunlight for the first 3 to 4 days and kept it under the shade for the remaining drying period, which was not less than 28 days.

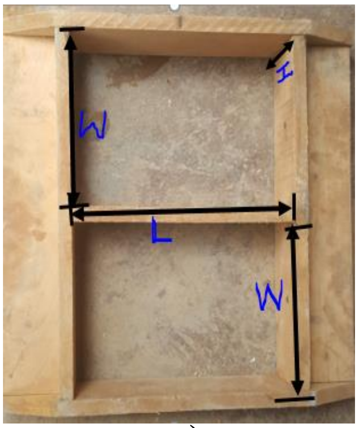


a) b) c)

d)

Figure 4-5 a) Wooden mould, b) casting of adobe c) removing the mould d) drying

4.5 Compression prism specimen Preparation

The specimen block was cured for 45 days, the first four days in the sun, and the rest in the shade of a compression prism made according to ASTM C1314-14 (ASTM 2014). Cutting the adobe in to two (**figure 4.5**), built (**figure 4.6**)and let it to dry at least for 28 days on the rack .

a.) cutting the full-size adobe in to two

Cutted the adobe in two two with size of 200X150X100mm each

Figure 4-6 preparing the prism by cutting the adobe in to two

b.) **Building the three-half adobe to a prism**

The adobe prism was constructed from three layers of adobe brick joined by 10 mm thick mortar of the same material composition .

Figure 4-7 construction of the adobe prism

c) **Drying the compression prism**

The compression adobe prism was dried on the rack under the shade with humidity between 47% and 97% and a temperature of 10.70 °C–23.40 °C for 64 days.

While the research by (Vandna 2015) proved that the strength varied up to 28 days of curing, the specimens of 28, 56, and 90-days of age were found to have the same compressive strength and, comparatively, more than those of 7- and 14-days of curing age.

Table 4-1 Specifications of compression prisms

Three layers of adobe bricks (horizontal stack)	
Dimensions	150mm x 200mm x 255mm
Specimen age (at testing) ~	64 days
Mortar thickness ~	10 mm
Average specimen height (H)	236mm
Average H/W ratio	1.66
Specimen drying condition	Air/sun dried on plastic surface.
	Temperature range :10.7°C – 23.4°C.
	Humidity range :47%-97%.
Drying load	none
Specimen quantity	25 prisms fabricated 5 prisms for each type of mix
Specimen weight	9.145 – 11.66kg
Average specimen density	1,738 kg/m^3

d)Transporting the compression prism to testing lab

According to ASTM C1532, packed two prisms in one cartoon package from the production site, was transported about 6km to the laboratory. Styrofoam had been used to partition the prism unit from colliding with each other.

e) Capping the compression prism

Before testing the prism, the top and bottom parts should be smoothened to distribute the pressure throughout the total area. So, according to ASTM C1552, spread the gypsum cement capping material evenly on the capping plate (or casting plate if used) that has been lightly coated with oil to detach from the capping plate easily (ASTM 2002).

Figure 4-8 Prisms capped ready for Compression Test

4.6 Investigation of the response of adobe Prism to compressive loading

4.6.1 Testing appliances and method

The compressive strength of the adobe prism specimen was measured using a universal testing machine (UTM 70-C0820/C). Figures 4-8a-c and 4-9 show how a CLF-IMNA type load cell and Linear Variable Differential Transducers (LVDTs) are linked to the TDS-630 Datalogger to monitor axial load and deformation, respectively.


a)


b)

c)

Figure 4-9) a) CLF-IMNA type Load cell b) TDS- 630 Data loger c) UTM 70-C0820/C

4.6.1.1 compressive strength and Stress–strain behavior

The set-up of the devices and input variables was chosen, like correction factors, must be investigated to address the correct compressive strength and the stress-strain behavior of the specimen.

4.6.1.2 deformation measuring device Installation

The installation of the measuring devices has an effect on the reading of stress-strain curves owing to the differential densification of the prism at different heights when axial compressive loading is applied. As shown in Figures 4-9, the strain measured by F-3 LVDTs (from the top) is not reliable due to the initial relative movement of the steel plate beside densification. This is indicated in Figure 4-9 c), where the Stress-strain curves for axial compression tests on adobe prisms, modified from (Blondet and Vargas 1978) F-1 and F-2 refer to the lateral LVDTs, while F-3 refers to the upper LVDTs.

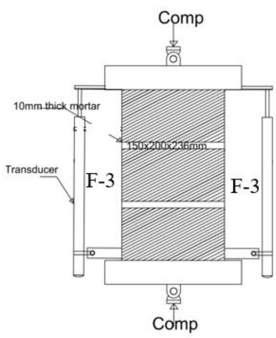

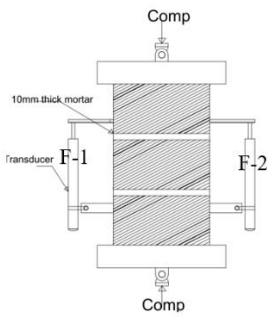

a) upper LVDTs) adobe prism measuring setup b) lateral LVDTs) adobe prism measuring setup

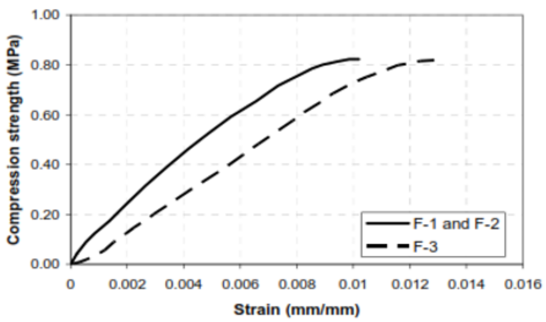

c) Stress Vs strain curves of Upper and lateral LVDTs set up

Figure 4-10 adobe prism measuring setup and their compressive strength Vs strain curves

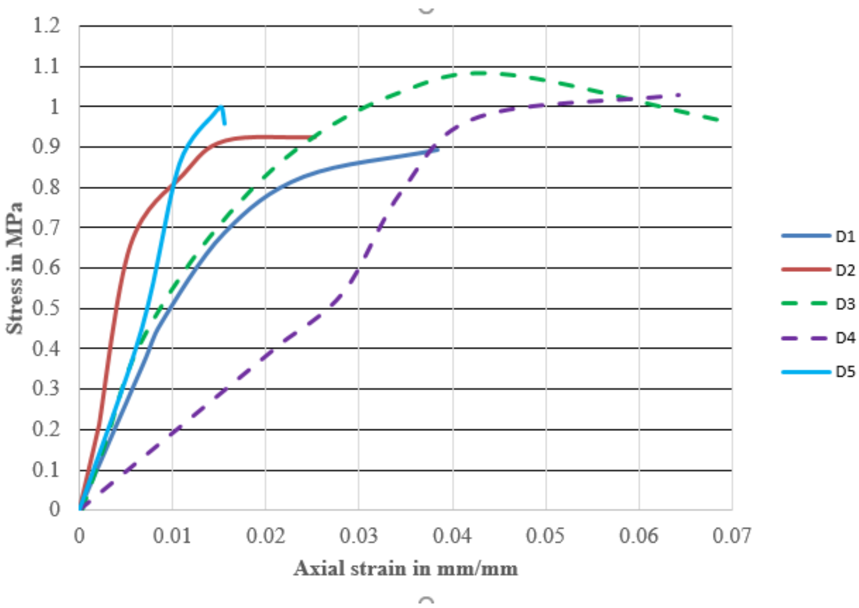

Figure 4-11 Specimen D adobe stress Vs Strain curve for different LVDTs set up

When the LVDTs in this thesis were configured as indicated in figure 4-9a, as upper LVDTs, the specimen (D3 and D4 of figure 4-10) shows steady longitudinal and transverse deformation than the lateral set-up.

4.6.2 Adobe prism compression test

A compression test is a test performed by using appropriate testing equipment on specimens used to identify the strength of the materials. According to ACI 530.1-11/SCEA, there are two types of compression tests for masonry. This thesis has used the prism compression test and interpreted the result as follows.

Prism test

The objective of these tests was to compute the maximum compression strength, f, of the composite adobe and mortar, the elasticity modulus, E, and the strain at failure. In this thesis, only the adobe prism's uniaxial compression and axial deformation of the specimens are reported. After testing the Prism compression, the adobe prism with a high capacity of compression strength has been representative of the small-scale model.

a)**Calculation of compressive strength of specimen**

The compressive strength of the specimen shall be—

$f_{sp} = k_a(F_{sp}/A_d)$ . . ………………………………………… 4-1

where, f_{sp} = the unconfined compressive strength, in megapascals

k_a = the aspect ratio factor for the specimen

F_{sp} = the total load at which the specimen fails, in newtons

A_d = the combined bedded area and grout area, if any, of the specimen, in square millimeters (for ungrouted specimens, Ad = Ab), based on work size dimensions except that in the case of in-situ testing, the actual length shall be taken (Standards.Australia 2001).

Table 4-2 summarizes the average compression strength of all specimens and the stress-strain curve one for each mix ratio specimen tested as shown in Figures 4-11.

The mix design of specimen D has resulted in the highest unconfined compressive strength tested (see the detail of all specimens in Appendix A).

Table 4-2 Average Confined compression strength of specimen A-E

	Prism Strength fc (kPa)				
Prism	**A**	**B**	**C**	**D**	**E**
1	770.96	817.00	717.00	878.37	886.50
2	487.13	691.38	639.70	923.15	833.67
3	548.32	879.66	748.84	1,081.63	767.00
4	614.43	775.33	732.03	1,054.79	800.33
5	569.23	845.17	841.91	1,000.33	883.56
Average	598.01	801.71	735.90	987.66	834.21
SD	**95.68**	**64.91**	**64.86**	**76.94**	**46.55**
CoV (%)	16.00	8.10	8.81	7.79	5.58

Notes: SD = Standard Deviation , CoV = Coefficient of Variation

* Determine the aspect ratio correction factor from AS 3700

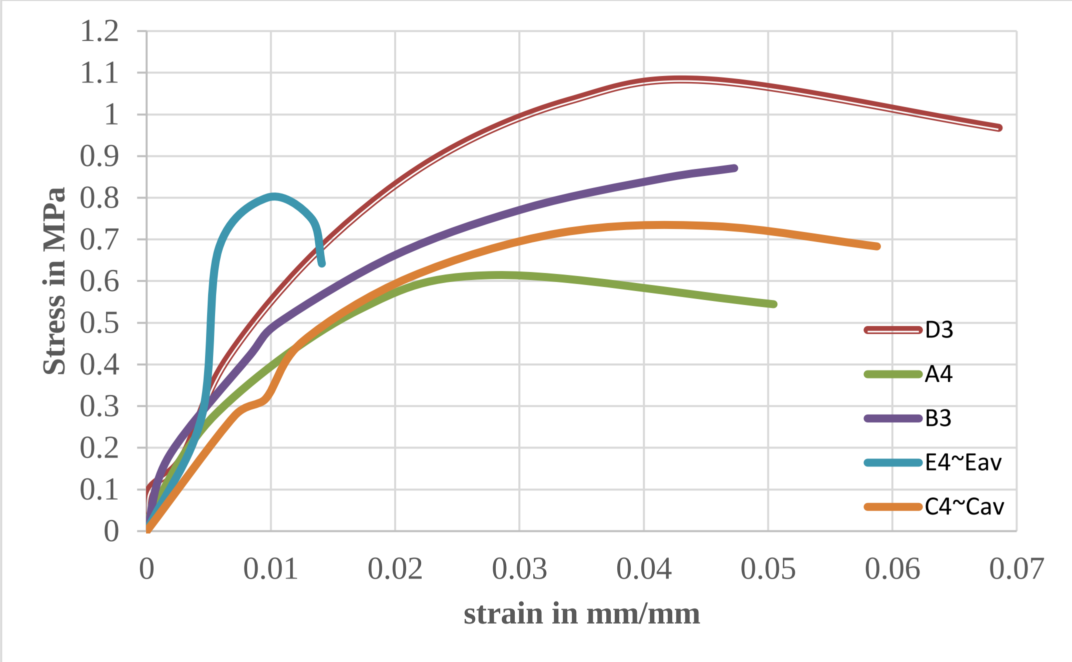

Figure 4-12 stress -strain curve of selected specimen from each mix design

b) Stress-Strain behavior of the adobe prism under uniaxial compression

The compression stress-strain behavior, recorded from the datalogger and the video, can generally be divided into three distinct stages, as shown in Figure 4-13, with some errors corrected.

In the initial stage, the contact adjustment will continue until the entire plate rests on the specimen surface, where the graph will be as shown in figure 4-13 (0-A); the specimen will also undergo consolidation at this point (A-B). It was discovered that consolidation occurred at a greater strain range in prismatic specimens (Rogiros, et al. 2014).

That's why an adjustment is made at the initial loading-deformation curve of this stage, approximately at the first 6–10 KN loading in this experiment. The graph shows a sudden consolidation and a large strain.

In the second stage (B-C), it has been observed that the development of the consolidation process causes further hardening of the prism, which makes the graph proportional (linear) before maximum stress is reached.

In the third stage (C-D), the material is subjected to compression softening once its maximum load-bearing capability is exceeded, up to the final strain sustained. Only in the case of cylinders and cubes was post-peak softening detected. Prisms were exposed to continual consolidation at the deformation levels studied (Rogiros, et al. 2014).

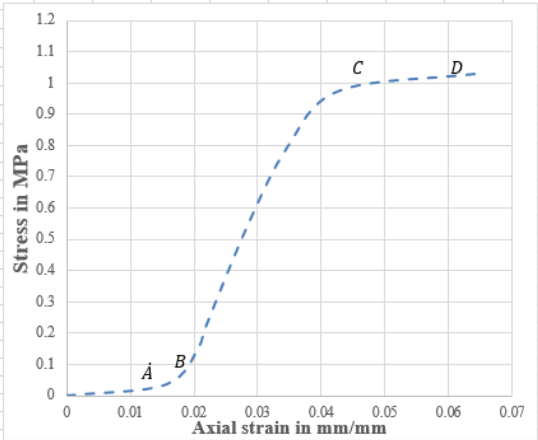

Figure 4-13 Stress-strain curve of specimin D4

The configuration of the deformation set-up, the transducer, affects the stress-strain curve as described in figures 4-9 and 4-10 also.

c) Elasticity modulus /Young's Modulus /

The elasticity modulus calculated for the adobe specimen D by incorporating different calculations methods described below shows similar results.

N.B. The curve shown in figure B-1,Appendix B represented specimen D's stress strain after the initial consolidation were adjusted.

i) Young's modulus according to ASTM E111-04

Young's modulus is the ratio of tensile or compressive stress to corresponding strain below the proportional limit.

By using the equation given in ASTM E111-04, Section 8.1 (2010), see Section 2.4.2.2 of the literature review.

Table 4-3 Young's modulus of elasticity

specimen	stress	strain	Em
D1	0.36	0.007	52.9
D2	0.21	0.002	99.19
D3	0.18	0.003	61.61
D4	0.15	0.0069	21.85
D5	0.45	0.007	67.16

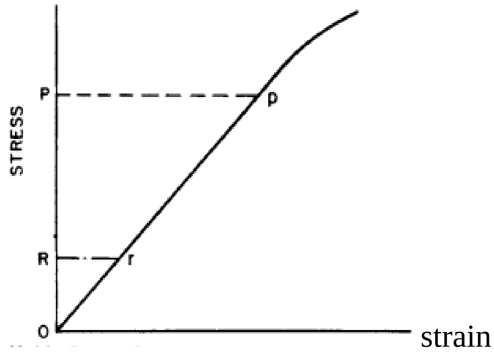

Figure 4-14 young's modulus according to ASTM E111-04

ii) Elasticity modulus according to (Blondet and Vargas 1978)

The elasticity modulus was calculated by taking 50% of the greatest compression load and its corresponding deformation from the elastic region of the stress-strain curve from the test recorded as shown in figure B-1 in Appendix B.

Table 4-4 Modulus of elasticity according to (Blondet and Vargas 1978)

specimen	stress	strain	Em (MPa)
D1	0.45	0.008456	52.90
D2	0.46	0.004654	99.19
D3	0.54	0.008345	64.81
D4	0.51	0.026945	19.07
D5	0.54	0.008068	67.16

iii)Chord modulus according to (ASTM-E111–04 2010).

The chord moduli of specimen D have been computed over the gradient of the curve by drawing a line that best fits the curve-increasing section of the stress-strain curves, which is between any two stresses. See the graph in figure B-1 in Appendix B.

The value obtained here varies a little bit from the above i) and ii)

Table 4-5 chord moduli according to ASTM E111-04 of specimen D

specimen	Chord moduli MPa
D1	23.96
D2	36.65
D3	25.43
D4	17.53
D5	67.88

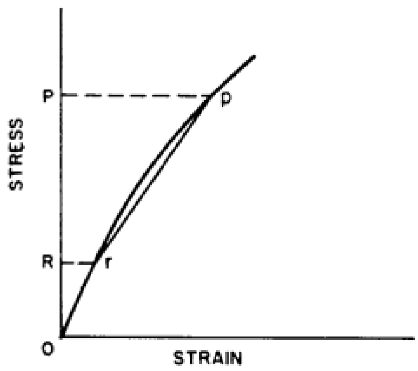

Figure 4-15 chord moduli according to ASTM E111-04

4.6.3 The mode of failure of the specimen

The crack pattern of the Adobe prism differs from one prism to another within the bounded threshold. The reason for this variation is the properties of the crack depending on the composition of the clay, sand, and straw that can vary in the same mixture.

According to (Sasuia and Jinwuth 2016) The maximum durability of specimens was found with the addition of straw since it improved the maximum stability of specimens in static water, reduced water absorption, and shrinkage more than rice husk.

Because adobe bricks and mortar were made of mud, an adobe wall can be assumed to be homogeneous and isotropic. The specimens responded monolithically to compressive loading, causing them to deform in both transversal directions.

crack width

maximum crack of width 2mm is observed on the specimine D5 which exibit the highest compression strength.

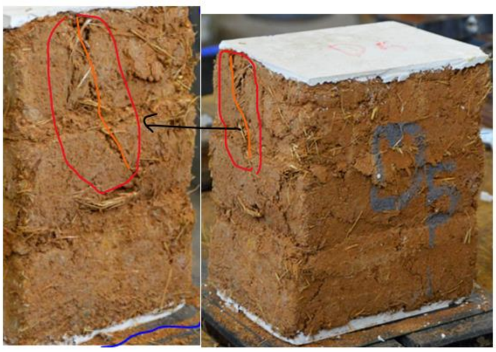

Figure 4-16 crack pattern and crack width of specimine D5

4.7 Analysis of the reduced scale adobe model

4.7.1 Reduced scale adobe specimen production

The small-scale adobe of size 10X6.6X5.6 cm3 was produced with the soil to straw ratio of the maximum compression strength specimen (D)result obtained in Table A-4 of Appendix A.

Figure 4-17 solid reduced scale specimens

4.7.2 Unit specimen compression testing result of the small scale adobe

The small scale adobe specimen is tested for compressive strength with a constant loading and the result has been recorded as shown in the Table 4.6 .

Figure 4-18 capping and testing of the reduced scale unit adobe

Table 4-6 unit compression strength of reduced scale adobe

specimen					
#	**size (mm)**	**Aspect ratio**	**Area (mm^2)**	**Force (N)**	**fc (N/mm^2)**
1	99X66X56	0.85	6534.00	6500.00	0.99
2	99X66X56	0.85	6534.00	6800.00	1.04
3	98.6X66X56	0.85	6507.60	6100.00	0.94
4	99X65X56	0.86	6435.00	8000.00	1.24
5	99X64X56	0.88	6336.00	6800.00	1.07
6	99X66X56	0.85	6534.00	6500.00	0.99
				Av	1.05
				Std	**0.10**
				Cov	9.28 %

4.7.3 Reduced scale adobe model construction

Specimen was built with a total of 437 small scale adobe bricks. The wall was constructed using the same process as specimen 3B of previous research (see the detail in section 2-5), with a wall thickness of 66mm. The wall specimen's height-to-thickness ratio (h/t) was 12.42, and the height-to-diameter (h/d) ratio was 0.68. Prior to testing, the specimen was cured for a minimum of 7 days after construction.

Figure 4-19 construction of the model

Figure 4-20 bottom and top side of roof of the model

4.7.4 Reduced scale adobe model testing using static tilt table

The specimen of this thesis was subjected to increasing roof load of 2.25,.3.75, 4.25 and 5.25 kN.

The 1st loading case tested tilted to an angle of 45^0 and there were no cracks observed. Hence the specimen was returned to the zero angle (initial position) and loaded with an additional loading for three more cycles as shown in the Table 4-7 and tilting angles in Table 4-8.

The specimen was uplifted at the heel and crushing at the toe in the 4th case loading with tilting angle reached 40^0 see figure C-4 in the Appendix C.

This kind of failure can be categorized under the in-plane walls failure mode due to the base of the foundation rigidity deteriorated being loaded beyond the assumed design load not the failure of the wall (it detaches from the base without a crack on the wall see figure C- 4 in the Appendix C).

Table 4-7 Small scale adobe models: specifications

Model Set	*Wall Thickness* (mm)	*Diameter (m)*	*Wall Height* (m)	*Roof Height* (m)	*Roof Load Pressure* (kN/m^2)	*Total Roof Load* (kN)	*Total wall load* (kN)
Previous 3B	**60**	**1.2**	**0.82**	**0.94**	**2**	**2.25**	**2.93**
This research 1st Load Case	**66**	**1.2**	**0.82**	**0.94**	**2**	**2.25**	**2.74**
2nd Load Case	**66**	**1.2**	**0.82**	**0.94**	**3.5**	**3.75**	**2.74**
3rd Load Case	**66**	**1.2**	**0.82**	**0.94**	**4.0**	**4.25**	**2.74**
4th Load Case	**66**	**1.2**	**0.82**	**0.94**	**5**	**5.25**	**2.74**

4.7.5 Comparative analysis of the static tilt table tests results

To compare the enhancement due to the mix design, the geometry of the specimen and the model were kept the same as the previous research described in **section 2-5 , Table 2-9 and Table 2-10**.

Table 4-8 Results of the circular specimen subjected to gradual increased loading to static tilt testing

Load	***CASE #3B***	***CASE #1st***	***CASE #2nd***	***CASE #3rd***	***CASE #4th***
First crack Angle (degrees)	**32**	**Greater than 45**	**Greater than 40**	**Greater than 40**	**Greater than 40**
Horizontal force (*kN*)	**2.75**	**Greater than 3.53**	**Greater than 4.18**	**Greater than 4.49**	**Greater than 5.14**
horizontal force compared to model own weight (%)	**52.9**	**Greater than 70.71**	**Greater than 64.28**	**Greater than 64.28**	**Greater than 64.28**

Mode of Failure

The failure is one of the three common failure modes for in-plane walls: first, overall wall panel rocking, which causes uplift at the heel and crushing at the toe if the compressive load exceeds the compressive strength of the wall material but here it is due to the weak foundation of the base of the wall which is soft earth cannot form monolithic or even fundamentally strong foundation restraint with the hard checkered steel plate.

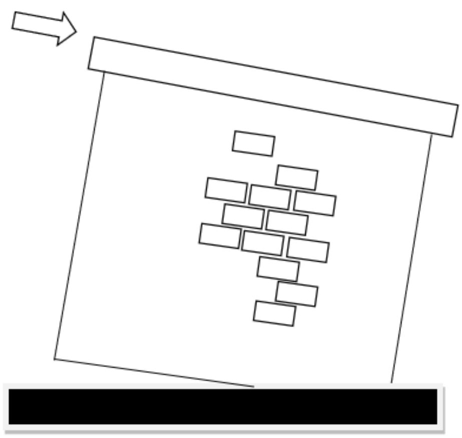

Figure 4-21 Rocking and uplift, toe detaching

Comparison of result with the previous research

This result at which the wall of the model stayed intact without a crack though the horizontal lateral force reaches 187% compared with the previous research as shown in Table 4-8.

This maximum result has been attained through selecting the appropriate mixture design of the adobe specimen. Besides the method and accuracy of constructing the wall has impact on the good result.

4.7.5.1 Capacity estimation of the adobe model using the static tilt table (Pseudo static analysis)

Here by relating the Pseudo static analysis with the static tilt table result of small scale (1:3) model construction obtained. The earth quake resistance capacity had been estimated as:

PGA= $K_h = a_o/g = \sin(\theta)$ .Where K_h =The horizontal pseudo static acceleration .

For the initial test i) 1st Case,

Given Tilted angle $\theta=45^0$, the equivalent PGA found was calculated as

Sin $\theta = \sin 45^0 = 0.707$, the peak ground acceleration, PGA=0.707, on an adobe model building with a roof load pressure of 2kN/m^2 and a wall load of 2.74 kN, according to the specification Table 4-7.

Similarly for the last test ii) 4th case

The model tilted $\theta=40^0$, the equivalent PGA was calculated as, $K_h=\sin 40^0=0.643$, PGA=0.643. For a model with roof load pressure of 5 KN/m^2 and wall load of 2.74 kN.

4.7.5.2 Capacity estimation of the adobe prototype from the similitude requirements

Converting the small scaled result into the prototype from similitude requirements, the Scale factor Sr, ($Sr=r_m/r_p$, r will be the properties like length, l, elastic modulus E etc.) for concentrated and surface/ pressure loads are $S_E S_L^2$ and S_E respectively (Harris and Sabnis 1999).

The static behavior of the structure can be described by two basic quantities, the geometrical scaling parameter S_L,and the scaling parameter of the elastic modulus S_E.

Since both the model and prototypes are in the same gravity field, the two basic similarity laws can be given in the following equations.

$S_{\sigma}= S_{\rho}\ S_{L} = S_{E}$, ………from the similitude requirement Table 2-14

Since it was considered that the same material was to be used for the model and the prototype, the density of the model and the prototype was assumed to be the same,

S_{ρ} =1 and the equation will be reduced to

$S_{\sigma}= S_{E} = S_{L} = \frac{\sigma_{M}}{\sigma_{p}}, \sigma_{P}=\frac{\sigma_{M}}{S_{L}}$ =3*2=6kN/m^2, for 2kN/m^2 model,

and =5*3=15 kN/ m^2 for the last case of 5kN/m^2 model roof pressure.
The capacity of the prototype for total wall load (Fp), for Scale factor Sr= $S_E S_L^2$

$S_{\sigma} = \frac{S_F}{S_L{}^2} = S_E$ ………… from the similitude requirement Table 2-14

$\frac{F_M}{F_p}=S_L{}^2 S_E$, $F_p = \frac{F_M}{S_L{}^2 S_E} = \frac{2.74}{(1/3)^2}$=24.66kN

The scale factor for acceleration of the model and prototype is 1 (Mooncarz and Krawinkler 1990).

5 CONCLUSIONS AND RECCOMENDATIONS

5.1 Conclusion

From the research output, the non-probably sampled raw soil (58.82% of sand,23.18% of silt and 18% of clay,with an average moisture content of 19%) proved that its mixture with the teff straw 'chid' with a ratio of 2:1 by volume, respectively, resulted in the maximum strength among the other five combinations of the raw soil blended with sand and chid.

The 1/3 reduced scale adobe model, built with adobe block of size 100X66X56 mm^3 and tested from this mixture design (2:1), has resisted the horizontal lateral force more than 187% to the previous research without a crack, though it can resist more if the base restraint is designed well. This maximum result has been attained through selecting the appropriate mixture design of the adobe specimen, besides the method and accuracy of constructing the wall which has a considerable impact on the result.

From the results obtained, it is feasible to build an adobe structure that has a wall load of 24.66 kN and a roof pressure of 6 kN/m^2 that withstands a seismic with a PGA of 0.71. And also, with the same wall load but a roof pressure of 15kN/m^2, it can withstand a seismic PGA of 0.643. The maximum capacity of the roof load hints that the adobe can be built a story or more up.

We can conclude that the mix design gives significant results, which can popularize adobe brick, which is abundant, cheap, eco-efficient, sustainable, low fire risk, virtually soundproof, and has better thermal capacity in hot or cold weather. Furthermore, adobe avoids the adapted use of wooden reinforcement for mud buildings, which reduces deforestation. Lastly, it is an environmentally friendly product that reduces carbon footprint. As the scarcity of construction materials escalates, green buildings like adobe brick will become inevitable.

5.2 Recommendation

The finding of the study indicates that there is a significant gap between the

- Standard method of production of the test specimen to attain constant coefficient of variation on the result.
- Design of the foundation for models and prototypes of adobe buildings.
- Study on the possible standard size of the adobe brick to attain the maximum output.
- Geotechnical soil map of the selected location for the production of adobe brick.

REFERENCES

Al.Vasilescu. 1969. *Analiza dimensionala si teoria similitudinii.* Editura Academiei Republicii Socialiste România.

ASTM. 2014. *ASTM C1314-14 . Standard Test Method for Compressive Strength of Masonry Prism.* West Conshohocken: ASTM International.

ASTM. 2002. *ASTM C1552 -02 Standard Practice for Capping Concrete Masonry Units; Related Units and Masonry Prisms for Compression Testing.* West Conshohocken: ASTM International.

ASTM. 2010. *Standard Guide for Design of Earthen Wall Building Systems,ASTM Designation: E2392/E2392M − 10e1.* 100 Barr Harbor Drive: ASTM International, 100 Barr Harbor Drive.

ASTM-E111–04. 2010. *American Society for Testing and Materials : Standard Test Method for Young's Modulus, Tangent Modulus, and Chord Modulus .* ASTM International.

Bible, King James. n.d.

Blondet et al., Marcial. 2011. *Earthquake-resistant ConstruCtion of adobe buildings: a tutorial.* california: Earthquake Engineering Research Institute,.

Blondet, M., and J Vargas. 1978. *Investigación sobre vivienda rural.* Lima, Peru: Pontificia Universidad Católica del Perú.

Blondet, M., G. V. Garcia, and S. Brzev. 2003. *Earthquake-Resistant Construction of Adobe Buildings.* EERI/IAEE World Housing Encyclopedia (http://www. world-housing. net) .

Blondet, Marcial, and Gladys Villa Garcia. 2003. *,Earthquake Resistant Earthen Buildings.* California: EERI/IAEE world housing encyclopedia.

Calkins, Meg. 2009. *Materials for Sustainable Sites ,A Complete Guide to the Evaluation, Selection, and Use of Sustainable Construction Materials.* Hoboken, New Jersey: John Wiley & Sons, Inc.

Clifton, James R. 1977. *Preservation Of Historic Adobe Structures— A Status Report.* Washington,DC: U.S.department of commerce ,National Bureau of Standards.

Crocker, Edward. 2001. *Earthen Architecture and Seismic Codes;Lessons From the Field.* Crocker Ltd. Architectural Conservation,Trustee, US/ICOMOS.

Devnani, G.L., and Shishir Sinha. 2018. "African Teff Straw as a Potential Reinforcement in Polymer Composites for Light-Weight Applications: Mechanical, Thermal, Physical, and Chemical Characterization before and after Alkali Treatment." *Journal of Natural Fibers:Taylor & Francis.*

Dhandhukia, Pinakin, Dweipayan Goswami, Parth Thakor, and Janki N Thakker. 2013. *Soil property apotheosis to corral the finest compressive strength.* Elsevier Ltd.

Doat, P, A Hays, H Houben, S Matuk, and V Vitoux. 1991. *Building With Earth.* First English. Translated by :Manu Bhatnagar Asha Puri. New Delhi,: The Mud Village Society.

Dowling, D.M.: SamaliI, B.: LI, J:. n.d. "Seismic Improvement of Adobe brick Walls - Comparison Between internal and ExternalVertical Reinforcement."

Eyre, and T. A. 1935. *The Physical Properties of Adobe Used as a Building Material.* Vol. 1. 3 vols. Albuquerque,New Mexico: The University of New Mexico Bulletin, Engineering Series.

Feng, Wu, Hai-Tao Wang, Li Gang, Jin-Qing Jia, and Hong-Nan Li. 2016. "Seismic performance of traditional adobe masonry walls subjected to in-plane cyclic loading." *Materials and Structures* (Materials and Structures) 50: 1-14.

Feng, Wu, Li Gang, Li Hong-Nan, and Jia Jin-Qing. 2013. *Strength and stress–strain characteristics of traditional adobe block and masonry.* Materials and Structures 46:1449–1457. doi:DOI 10.1617/s11527-012-9987-y.

Hakimi, A, O Fassi-Fehri, H Bouabid, D Charif, S ouazzane, and M El Kortbi. 1999. "Non-linear behaviour of the compressed earthen block by elasticity-damage coupling." France: Materials and Structures . 539–545.

Harris, H.G, and G.M.: Sabnis. 1999. *Structural Modeling and Experimental Techniques.* CRC Press.

Hesham, El-Emam Hani, Salim Stephen, Robert Pigg, Gabriela Saucier, and Aaron. 2018. "Structural Characterization and Blast Response of Adobe Walls." *Structures Conference.* American Society of Civil Engineers. 383-391.

Houben, H., and H.: Guillard. 1994. *Earth Construction: A Comprehensive Guide.* London: Intermediate Technology Publications.

Jazar, Reza N. 2020. *Approximation Methods in Science and Engineering.* New York: Springer Science+Business Media, LLC, part of Springer Nature.

Jinwuth, Watcharin. 2012. "Study into the Earthquake Resistance of Circular Adobe Buildings using Static Static tilt Tests." Perth, Western Australia.

Jinwuth, Watcharin. 2012. *Study into the Earthquake Resistance of Circular Adobe Buildings using Static Static tilt Tests.* Perth, Western Australia: Doctoral Dissertation.

Kitch, William A. 2009. *Geotechnical Engineering Lab Manual.* Kendall Hunt publishing company.

Kouakou, CH, and JC Morel. 2009. "Strength and elasto-plastic properties of non-industrial building materials manufactured with clay as a natural binder. ;." Applied Clay Science. 27–34.

Lisa Schroder, and Vince Ogletree. 2010. *Simple, Affordable, and Earthquake-Resistant Natural Building Techniques.* White river junction,vermont: Chelsea publishing.

Meyer, CS : Chalivendra, V: Song, B:Casem, and D :. 2013. "Numerical simulations of the mechanical behavior of adobe." New York: Proceedings of the 2012 Annual Conference on Experimental and Applied Mechanics.

Minke, G:. 2001. *Construction manual for earthquake-resistant houses built of earth.* Accessed April 01, 2019. <http://www.gtz.de/basin>.

Monica Nicoreac et al. 2010. "Similitude theory and applications." *Acta Technica Napocensis: Civil Engineering & Architecture Vol. 53, No. 1, (2010).*

Mooncarz, Potra D., and Helmut Krawinkler. 1990. *theory and application of experimental model analysis in earthquake engineering by.* The John A.Blume Earthquake Engineering Center.

Morel, JC. : Pkla, A : Walker, P. :. 2007. "Compressive strength testing of compressed earth Blocks." *Construction Building Materials;21:* 303–9.

Pacheco-Torgal, F.:. 2015. *Eco-efficient Masonry Bricks and Blocks: Design, Properties and Durability.* Oxford: Woodhead Publishing.

Quagliarini, Enrico, and Stefano Lenci. 2010. *The influence of natural stabilizers and natural fibres on the mechanical properties of ancient Roman adobe bricks.* J. Cult. Heritage. doi:https://doi.org/10.1016/j.culher.2009.01.006.

Rogiros, Illampas, Ioannou Ioannis, Dimos, and C. Charmpis. 2014. *Adobe bricks under compression: Experimental investigation andderivation of stress–strain equation.* Construction and Building Materials.

Rogiros, Illampas: Ioannis,Ioannou:Dimos C., Charmpis. 2014. *Adobe bricks under compression: Experimental investigation and derivation of stress–strain equation.* Construction and Building Materials.

Sabino, Nicola, and Ruíz: Tarque. 2011. *Numerical modelling of the seismic behaviour of adobe buildings.* Ph. D. Dissertation , University of Pavia.

SADC. 2006. "Confined Masonery." *the trainings at the Housing Reconstruction Centres* . the Swiss Agency for Development and Cooperation.

Samali, B, DM Dowling, and J Li. 2015. "Static and dynamic testing of adobe-mudbrick structures." *Australian Journal of Structural Engineering* (Centre for Built Infrastructure Research, Faculty of Engineering, University of Technology Sydney, NSW) 8: 159-170.

San, A.: Bartolomé, A.: Quiun, and D.:. 2013. *Experimental research and seismic design proposal for confined adobe masonry.* 12 th Canadian Masonry Symposium Vancouver.

Sasuia, Sasui, and Warcharin Jinwuth. 2016. "Comparing the Effects of Straw and Rice Husk on the Durability of Mud Brick." *5th International Conference on Energy.*

Standards.Australia. 2001. *Australia Standard AS 3700-2001(Standards Australia 2001).* Standards Australia 2001.

Steen, Charlie. 1971. “An Archaeologist's Summary of Adobe.” *El Palacio* 77: 29-38.

Swan, et al A. Jenkins. 2011. *Sustainable Earthen and Straw Bale Construction in North American Buildings: Codes and Practice.* Journal of maerials in Civil Engineering,ASCE.

Tayyibi, Bouabid Mohammed, Zerouaoui Hamid, d'Ouazzane Jamal, and Charif, Cherraj Saad. 2016. *Security Requirements for earth construction:Comparative study of international codes.* J. Mater. Environ. Sci. 7 (7).

Tipler, J.F, M.L Worth, H.W Morris, and Q.T Ma. 2010. “Shake table testing of scaled geogrid-reinforced adobe wall models.” *NZSEE Conference.* Auckland: University of Auckland.

Vandna, Sharma : Hemant ,K.Vinayak : Bhanu M. :Marwaha. 2015. “Enhancing sustainability of rural adobe houses of hills by addition of vernacular fiber reinforcement.” *International journal of sustainable built environment* 4: 348–58.

Walker, P. 1995. “Strength, durability and shrinkage characteristics of cement stabilised soil blocks.” *Cement and concrete composites* 17 (4): 301-310.

Walker,P. 2002. *The Australian Earth Building Handbook, Standards Australia.* Sydney: Standard Australia International Ltd.

APPENDIX A Compressive strength of adobe prism

Table A-1 Result of compression strength of specimen C

Ka	AS 3700-2001 0.75				
Specimen A	**H/t Ratio**	**Surface Area (m^2)**	**Max Load P (kN)**	**Prism Strength fc (kPa)**	**Unconfined Compressive Strength* (kPa)* (AS 3700-2001)**
A_1	1.62	0.03	23.3	770.96	577.00
A_2	1.76	0.03	14.76	487.13	364.58
A_3	1.58	0.03	17.76	548.32	410.37
A_4	1.60	0.03	19.76	614.43	459.85
A_5	1.67	0.03	17.76	569.23	426.02
Average	1.65	0.03	18.67	598.01	**447.56**
SD	**0.06**	**0.00**	**2.81**	**95.68**	**71.61**
CoV (%)	3.87	2.89	15.07	16.00	**16.00**

Table A-2 Result of compression strength of specimen B

Ka	AS 3700-2001 0.75				
Specimen B	**H/t Ratio**	**Surface Area (m^2)**	**Max Load P (kN)**	**Prism Strength fc (kPa)**	**Unconfined Compressive Strength* (kPa)* (AS 3700-2001)**
B_1	1.67	0.03	24.51	817.00	611.32
B_2	1.65	0.03	21.26	691.38	517.33
B_3	1.62	0.03	25.51	879.66	658.20
B_4	1.60	0.03	23.26	775.33	580.14
B_5	1.68	0.03	24.51	845.17	632.40
Average	1.64	0.03	23.81	801.71	**599.88**
SD	**0.03**	**0.00**	**1.46**	**64.91**	**48.57**
CoV (%)	1.74	2.25	6.14	8.10	**8.10**

Table A-3 Result of compression strength of specimen C

Ka	AS 3700-2001				
	0.74				
Specimen C	**H/t Ratio**	**Surface Area (m^2)**	**Max Load P (kN)**	**Prism Strength fc (kPa)**	**Unconfined Compressive Strength* (kPa)* (AS 3700-2001)**
C_1	1.566667	0.03	21.51	717.00	532.15
C_2	1.601307	0.03	20.26	639.70	474.78
C_3	1.53125	0.03	25.76	748.84	555.78
C_4	1.566667	0.03	22.51	732.03	543.31
C_5	1.546667	0.03	25.51	841.91	624.86
Average	1.56	0.03	23.11	735.90	**546.17**
SD	**0.02**	**0.00**	**2.18**	**64.86**	**48.14**
CoV (%)	1.51	5.06	9.45	8.81	**8.81**

Table A-4 Result of **compression strength of specimen D**

Ka	AS 3700-2001				
	0.75				
Specimen D	**H/t Ratio**	**Surface Area (m^2)**	**Max Load P (kN)**	**Prism Strength fc (kPa)**	**Unconfined Compressive Strength* (kPa)* (AS 3700-2001)**
D_1	1.60	0.03	27.01	878.37	658.85
D_2	1.52	0.03	27.51	923.15	692.44
D_3	1.72	0.03	33.26	1,081.63	811.31
D_4	1.76	0.03	29.26	1,054.79	791.18
D_5	1.72	0.03	30.01	1,000.33	750.33
Average	1.67	0.03	29.41	987.66	**740.82**
SD	**0.09**	**0.00**	**2.22**	**76.94**	**57.71**
CoV (%)	5.34	3.70	7.54	7.79	**7.79**

Table A-5 Result of compression strength of specimen E

	AS 3700-2001				
Ka	0.75				
Specimen E	**H/t Ratio**	**Surface Area (m^2)**	**Max Load P (kN)**	**Prism Strength fc (kPa)**	**Unconfined Compressive Strength* (kPa)* (AS 3700-2001)**
E_1	1.65	0.03	27.26	886.50	663.53
E_2	1.6	0.03	25.01	833.67	623.99
E_3	1.68	0.03	23.01	767.00	574.09
E_4	1.58	0.03	24.01	800.33	599.04
E_5	1.71	0.03	24.51	883.56	661.33
Average	1.65	0.03	24.76	834.21	**624.40**
SD	**0.05**	**0.00**	**1.41**	**46.55**	**34.84**
CoV (%)	2.88	3.44	5.71	5.58	**5.58**

Notes: SD = Standard Deviation , CoV = Coefficient of Variation

* Determine the aspect ratio correction factor from AS 3700

Appendix B Modulus of elasticity

Figure B-1 Chords modulus of specimen D(D1-D5)

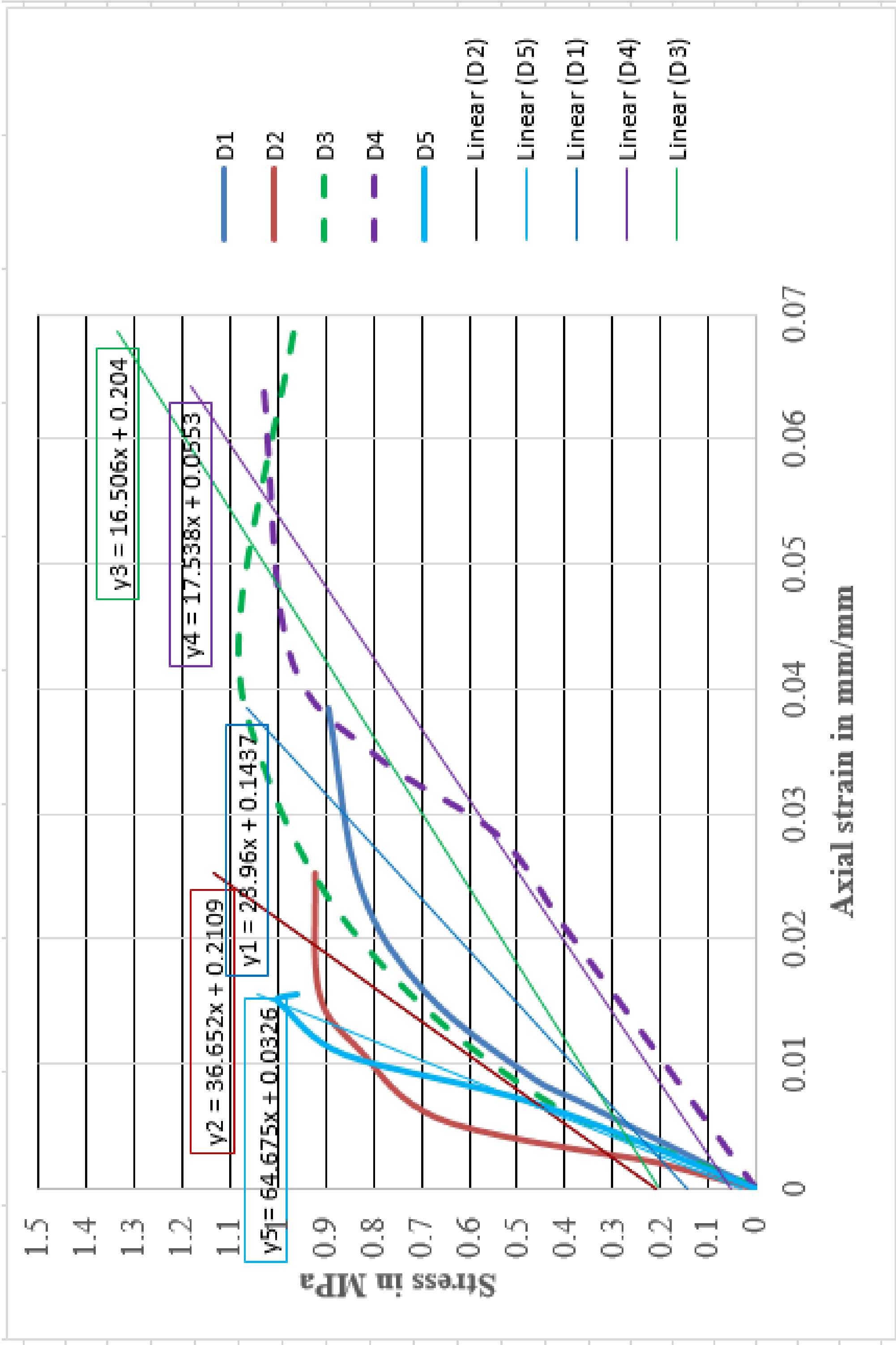

APPENDIX C Static Tilt Table Test Pictures

Figure C-1 **1st Case loading tilting the circular adobe model**

Figure C-2 2nd case loading tilting the circular adobe model

Figure C-3 **3rd Case tilting the circular adobe model with an addition of load and no crack is seen**

Figure C-4 4th Case loading **tilting the circular adobe model with an addition of load and no crack is seen but the toe detaching is observed**

Figure C-5 the model after the base detached